SIMULATION OF HEAT FLOW IN A DIRECT-CHILL CASTER USING COMSOL MULTIPHYSICS

LEE WEI LOON

Report submitted in partial fulfilment of the requirements

for the award of the degree of

Bachelor of Engineering (Hons.) in Mechatronics Engineering

Faculty of Manufacturing Engineering

UNIVERSITI MALAYSIA PAHANG

June 2016

UNIVERSITI MALAYSIA PAHANG

FACULTY OF MANUFACTURING ENGINEERING

EXAMINER'S DECLARATION

I certify that the project entitled **"SIMULATION OF HEAT FLOW IN A DIRECT-CHILL CASTER USING COMSOL MULTIPHYSICS"** is written by Lee Wei Loon. I have examined the final copy of this thesis and in my opinion; it is fully adequate in terms of scope and quality for the award of the degree of Bachelor of Engineering (Hons.) in Mechatronics Engineering. I herewith recommend that it be accepted in partial fulfilment of the requirements for the degree of Bachelor of Engineering (Hons.) in Mechatronics Engineering.

DR. NANANG FATCHURROHMAN

Examiner Signature:

SUPERVISOR'S DECLARATION

I hereby declare that I have checked this thesis and in my opinion, this thesis is adequate in terms of scope and quality for the award of the degree of Bachelor of Engineering (Hons.) in Mechatronics Engineering.

Signature :

Name of supervisor : ASSOC. PROF. DR. A.K. PRASADA RAO

Position : ASSOCIATE PROFESSOR

FACULTY OF MANUFACTURING ENGINEERING

UNIVERSITI MALAYSIA PAHANG

Date : 29 APRIL 2016

STUDENT'S DECLARATION

I hereby declare that the work in this thesis is based on my original work except for quotations and citations which have been duly acknowledged. I also declare that is has not been previously or concurrently submitted for any other degree at Universiti Malaysia Pahang or any other institutions.

Signature :

Name : LEE WEI LOON

ID Number : FB12049

Date : 29 APRIL 2016

Dedicated

To

My Beloved Parents

Father: *Mr. Lee Keat Sin*

&

Mother: *Mrs. Chua Siew Fong*

And To

My Respected Supervisor

Assoc. Prof. Dr. A. K. Prasada Rao

ACKNOWLEDGEMENTS

First of all, the author, I would like to express my deepest and sincere gratitude to my supervisor, Assoc. Prof. Dr. A.K. Prasada Rao for being my research advisor, for his guidance, perseverance and appreciation of my work throughout the research in this project. He has inspired me to be determined, never give up until I have achieved my goal and to become an enthusiastic person. I appreciate his consistent support from the first day I work with him. His outstanding professional conduct and ability to tolerate my naive mistakes has impressed me and become one of the most influential people in my life.

Further, I would like to acknowledge my appreciation to our final year project coordinator, Dr. Noor Mazni Binti Ismail, she also as my panel of my project presentation evaluator. Thanks for her dedication and support for all the final year students in Faculty of Manufacturing Engineering (FKP), so that we able to complete our task within the specified timeline. Many special thanks go to Dr. Nanang Fatchurrohman for his precious comments during my project presentation and also as my thesis examiner, which was crucial for me to overcome the challenges and to success.

Last but not least, I would like to thanks to my lovely mother, father, sister and my partner for all the love, dream, and sacrifice throughout my life, thanks for their support, perseverance, love and tender solicitude. I appreciate their tolerance and understanding for making my achievements possible. Without them, I would not be the person I am today.

LEE WEI LOON

ABSTRACT

Melt-conditioned direct chill (MC-DC) casting process is a novel billet casting technology developed recently for enhanced the grain refinement of cast billet without any grain refiner required. Present work endeavours to understand the behaviour of various parameters of rotor-stator based shearing device on the liquid above the solidification front of AZ31 Mg-alloy billet casting process. It has been found that the influence of increasing rotor speed on the extremely high casting speed has still remained unknown and no one has studied the effect of device diameter and depth of immersion on the billet temperature sump profile. In this work, industrial scale models of both the conventional direct chill (DC) and the (MC-DC) processes were generated by using COMSOL Multiphysics software, in order to study the effect of various parameters on the rotor-stator device for the first time. The results have revealed that the billet temperature distribution in the liquid sump profile is minimized significantly in that case of MC-DC model compared to the conventional DC model. This approach also investigated and revealed the effect of device diameter and depth of immersion of device on the temperature gradient of sump profile. The simulation results can predict the outcome based on various parameters and this is very useful in order to optimize the parameters for maximizing the cast billet quality and improve production line for the industry.

ABSTRAK

Process penuangan, pencairan dingin dan sejuk langsung ataupun (MC-DC) adalah teknologi alternative yang baru dibangunkan untuk meningkatkan penghalusan saiz butiran mickrostruktur dalam pemutus billet tanpa memerlukan sebarang penghalus butiran mikrostruktur. Kajian ini telah dijalankan untuk mengkaji dan memahami tingkah laku pelbagai parameter rotor-stator berasaskan peranti ricih pada cecair di atas depan pemejalan AZ31 Mg-aloi ketika proses tuangan. Hal ini telah mendapati bahawa pengaruh kelajuan rotor yang semakin meningkatkan pada kelajuan pemutus yang sangat tinggi masih kekal tidak diketahui dan tiada pernah mengkaji kesan diameter peranti ricih dan kedalaman rendaman peranti ricih mengenai profil bah suhu billet. Ini adalah kali pertama, model untuk proses sejuk terus tuangan konvensional atau (DC) dan model bagi MC-DC, kedua-dua model diwujudkan and dibina dengan menggunakan perisian COMSOL Multiphysics, supaya kajian kesan mengikut pelbagai parameter pada peranti ricih rotor-stator dapat dijayakan. Selain itu, hasial kajian telah menunjukkan bahawa suhu berada di dalam profil bah dapat dikurangkan dengan ketata dalam kes MC-DC berbanding dengan model DC konvensional. Kajian ini juga mendedahkan kesan diameter peranti dan kedalaman rendaman peranti pada kecerunan suhu profil bah dalam billet. Hasil kajian simulasi tersebut dapat meramalkan hasil berdasarkan pelbagai parameter dan ini adalah sangat bermanfaat untuk mengoptimumkan parameter supaya mampu memaksimumkan kualiti billet dan memajukan process pengeluaran dalam industri.

TABLE OF CONTENTS

CHAPTER 2 LITERATURE REVIEW

CHAPTER 3 METHODOLOGY

LIST OF TABLES

LIST OF FIGURES

LIST OF SYMBOLS

℃	Celsius
J	Joule
K	Kelvin
kg	Kilogram
m	Metre
mm	Millimetre
min	Minute
sec	Second
$\dot{m}$	Mass flow rate
ρ	Density
v	Velocity of the system
V	Average flow velocity
A	Cross-sectional area
E_k	Kinetic energy
m	Mass of an object

Q	Volume Flow rate
A_1	Cross-sectional area of the large device
A_2	Cross-sectional area of the small device
V_1	Average flow velocity of the liquid in the large device
V_2	Average flow velocity of the liquid in the small device

LIST OF ABBREVIATIONS

2D	2-Dimensional
3D	3-Dimensional
Al	Aluminium
AZ31	Magnesium Alloy
CFD	Computational Fluid Dynamics
DC	Direct Chill
FEA	Finite Element Analysis
H_2O	Chemical formula of water
HPDC	High Pressure Die Casting
MC-DC	Melt-Conditioned Direct Chill
MCAST	Melt Conditioning by Advanced Shear Technology
Mg	Magnesium
rpm	Revolution per minute
Zn	Zinc

CHAPTER 1

INTRODUCTION

1.1 PROJECT BACKGROUND

Direct chill (DC) casting process is a semi-continuous casting approach which was first established in the 1930s. It is a widely used technology in non-ferrous metallurgy especially to produce wrought Al-alloy and Mg-alloy billets. During the casting and post casting, there are many challenges which are to be overcome, such as bleed-outs, hot-tears, cold-shuts, macrosegregation etc. **[1,2]**. Research was done to resolve the problems like hot-tears and macrosegregation. Those methods were melt-conditioned direct chill (MC-DC) casting and electro-magnetic stirring technique **[3-10]**. The integration of these techniques in the conventional casting process (DC) has brought a promising improvement in the grain refinement and solute distribution of the cast billet which lead to a better cast quality.

Recently, magnesium alloy has been popularly being investigated for engineering applications such as light weight and energy saving engineering solutions. Undoubtedly, the demand on light weight alloy like magnesium billets is increasing gradually each year in electronics gadgets, automotive and aerospace industries **[25-28]**. Interestingly, some literature suggests that the solidification process is sensitive to the temperature gradient in the billet sump **[7-10]**. Therefore, the present research has been focused on the effect of various rotor parameters on the liquid sump profile temperature distribution in both DC and MC-DC casting process of Mg-alloy billets.

1.2 PROBLEM STATEMENT

The heat transfer in the DC casting will significantly influence the depth of the billet's sump profile which determines the quality of the cast billet. Recent research had presented that the extremely high casting speeds may not have a promising result of the grain refinement **[10]**, but the influence of increasing speed of rotor-stator device with the high casting speed has still remained unclear. In addition, the effect of rotor-stator diameter and device depth of immersion on the billet sump temperature profile has not been reported in the literature.

In this approach, a systematic modelling on MC-DC technique was developed at various rotor-stator speeds at different rotor diameter and depth of immersion of the shearing device in order to analyse the heat distribution. The 3D models of the AZ31 Mg-alloy billets with a solidification range of 80 ℃ at a fixed casting speed for MC-DC casters were created by using COMSOL Multiphysics software. Meanwhile, the influence of increasing speed of the rotor-stator device at different rotor diameter and depth of immersion in the casters have been justified by studying the temperature profiles of the billets by using COMSOL Multiphysics.

1.3 SIGNIFICANCE OF STUDY

For the several decades, the high quality of billets are of a major concerned. To minimize the defects, the research on MC-DC casting process has been focused recently. As researcher stated that the significant refined microstructure was noted without grain refiner additives. Furthermore, the kinetics of phase transformations was significantly enhanced with the use of the rotor-stator intensive shearing device in the case of MC-DC casting process **[7-10]**.

Moreover, the extremely high casting speeds may not have a promising results for the grain refinements, but the influence of increasing speed of the rotor-stator device on the extremely high casting speeds is still unclear **[10]**. Therefore, the simulation works on the AZ31 Mg-alloy billet is essential to figure out the relationship of the speed of the rotor-stator device and effect of various rotor parameters on the sump profiles. In addition, simulation is a crucial step in order to develop a rotor-stator high shear device in an optimum way before it can be applied to a real life industry application.

1.4 OBJECTIVES

The main objectives of this project are as below:

- To design and develop a model of direct chill caster that takes into account of fluid flow and heat transfer analysis by using COMSOL Multiphysics software.
- To investigate the relationship between the speeds of the rotor-stator shearing device and the heat flow in the direct chill caster.
- To study the effect of the rotor-stator diameter and the depth of immersion of rotor-stator device on the billet sump temperature profile.
- To determine the optimum range of the rotor speed for the given casting speed.

1.5 PROJECT SCOPE

In order to achieve the objectives of this project, the model of the DC caster must be created in the environment of COMSOL Multiphysics software to simulate the fluid flow and heat flow in it with specific casting speed and various rotor parameters such as rotor speed, device diameter and depth of immersion. Further analytical and numerical results are to be compared with the earlier work as reported in the literature.

CHAPTER 2

LITERATURE REVIEW

2.1 INTRODUCTION

In this chapter, the author was intended to review the journal that related to the project. The keywords such as conventional direct chill (DC) casting, melt conditioned direct chill (MC-DC) casting, heat flow, Mg-alloys, COMSOL Multiphysics simulation and modelling of heat transfer have been reviewed and discussed in order to achieve the objectives of the project.

2.2 CONVENTIONAL DIRECT CHILL CASTING (DC)

2.2.1 Background

Direct Chill casting, widely known as DC casting (herein termed as DC) was invented since 1936-1938 by W.Roth, VAW (Germany) and W.T. Ennor, ALCOA (USA), where it is a commonly used technology for the production of nonferrous alloy such as large ingots and round billets since late 1930's **[1,2,11]**. Nonferrous alloys like aluminium and magnesium are popularly preferred due to its light weight, strength and high corrosion resistance **[12]**. The application of direct chill casting on nonferrous alloy is still widely using in the aerospace and automotive industry because of its versatility and robust nature. The ingenuity skill of engineering in the history of DC casting invention always suited the demands of the industry as we all know that nowadays, all aluminium alloys follow by magnesium alloys are produced by this

technique of casting. In addition, the production technique for casting nonferrous metals such as aluminium, copper, magnesium and zinc has proved to be economically **[1,2,11].**

2.2.2 Heat Flow

DC casting is a semi-continuous casting technique that has been categorised in continuous casting processes where the molten liquid of metal solidifies under a continuous cooling condition. As shown in **Figure 2.1** is a schematic of a typical DC caster of nonferrous alloys **[15]**. DC casting process the ingots in uniform cross section, initially the molten melt of light alloys is poured into a water cooled mould (primary cooling), probably a cooper mould or aluminium mould and then casting under a direct cooling medium (secondary cooling) which is cooled water spray. At the beginning stage of casting, the open ended of caster cooled mould is closed initially with a dummy block or a starter block (tertiary cooling) to allow the cast to be fed according to its casting speed. As the solid moves out of the mould that hold by starter block, the molten melts is continuously fed into the mould opening and then contained by the water cooled mould (primary cooling) **[11,13]**.

The heat is released to the surrounding from the superheated molten metal, where the latent heat is released from the liquid-solid state phase transformation **[14]**. The solidification process begins at the water cooled mould, thereby the first solid shell of the alloy billet forms of heat (5 to 20%) is extracted through the primary cooling zone. Furthermore, the starter block is withdrawn accordingly to its casting speed by pulling away from the mould wall with the formed solid shell. After that, the billet is allowed the direct chill water spray on its shell surface to extract most of the heat (80 to 95%) at the secondary cooling stage when attained steady state conditions. The DC casting process continues until a billet with a desired length is produced **[11,13-15,28]**.

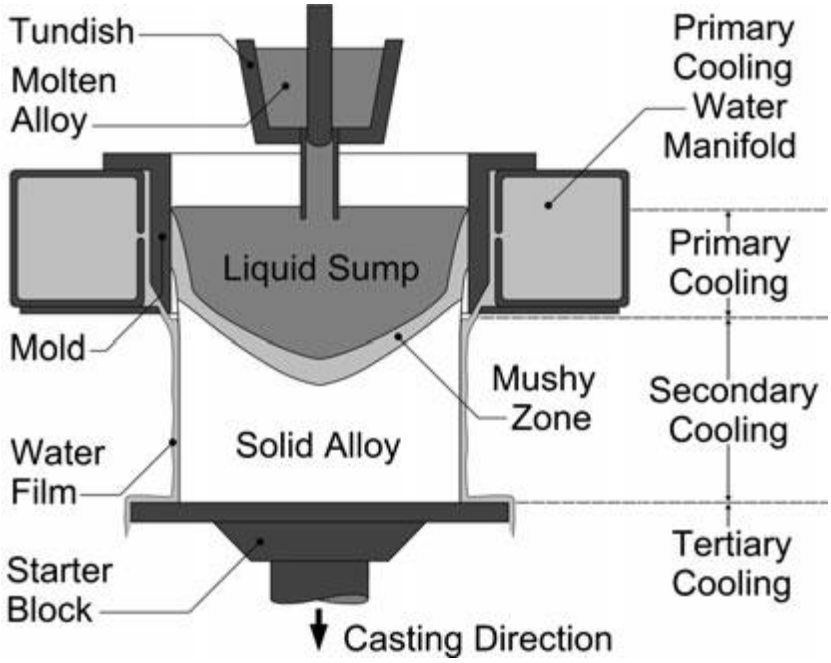

Figure 2.1: The schematic of a typical DC caster of nonferrous alloys **[15]**.
Source: Caron et al. (2012)

2.2.3 Defects

For the past few decades, the defects that occur on the solidifying alloys are inevitable. It has been an uphill task to deal with several of pre and post casting defects such as bleed-outs, hot-tears, cold-shuts, macrosegregation and etc. The non-uniform of chemical composition of the scale of molten melts during the DC casting, also called macrosegregation, which is one of the major defects that occurs during the casting process **[16,17]**. Macrosegregation occurs due to the difference concentrations of the alloys in the liquid phase and solid phase, thereby during the solidification of hypoeutectic alloys, the liquid phase appear with high concentration and the solid phase with less concentration. Therefore, the depletion of the solute in the casting process has led to the negative centreline segregation, hence consequent an irreversible defect that provide no choice to maintain the quality of billets but to manipulate during the very first casting stage. Based on the industry practice, literature stated that the deeper of the sump of the billet, the larger is the macrosegregation happen. Therefore, the casting parameters plays an important role in DC casting **[2,16]**.

Besides that, cold-shuts is considered another well-known defect, that is the shrinkage condition cause by the premature solidification in the mould during the primary cooling stage of DC casting of alloys billet **[2,10]**. Research had proven that the cold shuts will disappear as the casting speed increases from 140 to 200 mm/min for the DC casting process. The literature also suggests that the fluidity of the molten melts will be improved with the increase of the temperature gradient in the billet sump, as the cold shuts disappear when the casting speed increase **[10]**.

Furthermore, the bleed-out occur, when then solid shell during secondary cooling stage was fractured and the molten melts is bleeding out from the cast billet. It had suggested that by decreasing the casting speed in such a way that the billet was completely solidified in the whole cross-section during the primary cooling zone before it reach the direct chill region, the secondary cooling zone **[2]**.

In addition, hot-tears and porosity are also a popular defect that occurs during the solidification process of DC casting. The formation of hot tear is due to the inability of the material to withstand the thermal stress and strain within the solidification range, which eventually led to an uneven thermal contraction of a DC casting. It is more likely to occur in the mushy zone, which is the transition zone between liquidus and solidus due to shrinkage **[2,18,19]**. The review of Suyitno et al. also stated that the porosity and hot tear surface of DC cast billets was depending on the speed of cast **[18]**.

2.3 MELT-CONDITIONED DIRECT CHILL CASTING (MC-DC)

2.3.1 Background

Recently, several techniques were adopted in order to overcome the defects such as macrosegregation and hot-tears. Among the popular technique are melt conditioned direct chill casting (termed herein as MC-DC) and electro-magnetic stirring. Research had shown a significant improvement in the grain refinement and the solute distribution of the billet cast by using these techniques **[3-10]**. Moreover, (Hagheyeghi et al. 2010) also reported that this technique also improved the energy and cost savings, yet able to produce a high quality billet with uniform refinement of microstructure distribution **[20,39]**.

MCAST process (melt conditioning by advanced shear technology) is a prior solidification process that developed recent past from the novel technology. This technique is more preferred than electromagnetic stirring because the MC-DC is more efficient in the aspect of cost saving, produce high quality of the billet cast without adding any grain refiner and also the problems of macrosegregation and non-uniform microstructure have been resolved **[4,20]**. In **Figure 2.2**, illustrate the MCAST machine. This technique is the modification from the DC with an integration of a twin screw mechanism to generate a high shear rate and promote high turbulence flow rate to the molten melt, so that the solidification process is under intensive forced convection condition **[3,10]**.

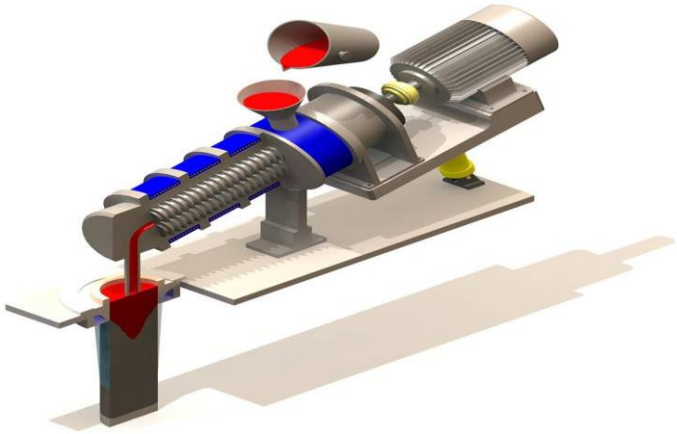

Figure 2.2: The schematic of a MCAST machine **[3]**.
Source: Haghayeghi, Liu and Fan (2008)

Besides the MCAST device, that is another way of developing melt-conditioned liquid metal, which is the MC-DC process. The process integrates the DC caster with a rotor based high shear device that immersed into the casting of the billet sump to control the in situ microstructure as shown in **Figure 2.3**. (Xia, Prasada Rao, & Fan, 2013) reported that this technique has the effects like: (1) disperse the oxides particle effectively which potent heterogeneous nucleation; (2) provide force convection flow at the solidification front and (3) the temperature of quasi-isothermal of the billet sump is just below the liquidus of alloys **[7]**.

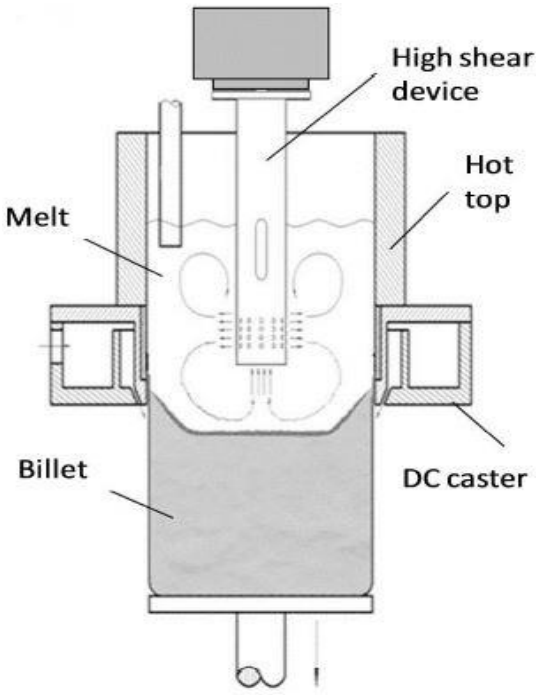

Figure 2.3: The schematic of MC-DC casting process with high shear device **[7]**.
Source: Xia, Prasada Rao and Fan (2013)

In the paper presented by (Haghayeghi, Liu, & Fan, 2008), the objective of authors was to investigate the effect of processing parameters on the microstructure and uniformity of composition of Al-alloys on series of 5754 and 7075 with the approached of both DC and MC-DC casting processes. The results has been confirmed that the DC cast billet have the typical 3-zone structure exhibits in it. Firstly, the chilled zone shown that with fine equiaxed grains at the outer surface of the billet. Then the centre of billet exhibit the coarse equiaxed structure, where in between the chilled zone and coarse equiaxed zone exhibits the columnar grains. However, the MC-DC billets cast is produced with fine and uniform in microstructure and the uniformity of chemical compositions also been achieved throughout the whole cross section of the billet cast, therefore, the cast defects like porosity and cracks were reduced significantly **[3]**.

2.3.2 Melt Conditioned Casting of Magnesium Alloys

The experiments were conducted by (Fan et al., 2009) in order to overcome the challenges of developing a solidification processing by ensuring an uniform and fine microstructure as-cast billet is free from macrosegregation and cast defects. The selection of light alloys are AZ91D with a liquidus of 597 ℃, melted at 700 ℃ then straight away fed into the melt conditioned unit for intensive shearing at 800 rpm under 605 ℃ for 45 seconds. Followed by, the conditioned molten metal was fed into a cold chamber for high pressure die casting (HPDC) for producing a standard shaped for tensile testing and microstructure characterisation. Interestingly, the outcome shown that the total porosity occur in melt conditioned high pressure die casting (MC-HPDC) samples is reduced compare to the conventional HPDC sample which contain higher amount of porosity. Moreover, no macrosegregation is reported as the alloying elements are uniformly distributed throughout the MC-HPDC sample. Therefore, the grain refinement is achieved without adding refiner additives in the melt conditioned technique. Furthermore, the mechanical properties of AZ91D alloys have come to a promising results, which was both strength and ductility of the melt conditioned samples are considerably higher that the sample produced by the conventional method. The literature's authors also summarized that the as-cast microstructure can be refine substantially through intensive high shearing technique and promote higher quality of billets **[4]**.

(Xia et al., 2013) also carried an experiment on commercial AZ31 Mg-alloys which was melted at 720 ℃ under a protective atmosphere (N_2 + SF_6) and fed into a DC caster at 695 ℃ under MC-DC process. The results shown that, with an intensive high shearing speed (5000 rpm), the sump of billet has been reduced, whereas, for the conventional DC process, the sump has a deep parabolic shape with 75 mm of depth. The literature also reported that the significant result of grain refinement in microstructure of AZ31 was observed. Instead of coarse dendritic grain of microstructure, the MC-DC casting with high shearing speed results in a fully fine rosette structure **[7]**.

2.3.3 Heat Flow

According to (Prasada Rao, 2014), an experiment was carried out based on the Al-6Zn alloy to observe the effect of the melt condition on the temperature of billet sump by two thermocouples T_1 and T_2 as illustrated in **Figure 2.4.** The hot top and the rotor stator were pre-heated to 735 ℃ and 750 ℃ respectively. The rotor stator was immersed in the billet sump where above the solidification front and was keeping switched OFF until steady state condition was achieved (DC). There was about 200 mm of the billet was cast at 250 mm/min, and then later, the shearing device was switched ON at the same casting speed (hereafter considered as MC-DC) **[9]**.

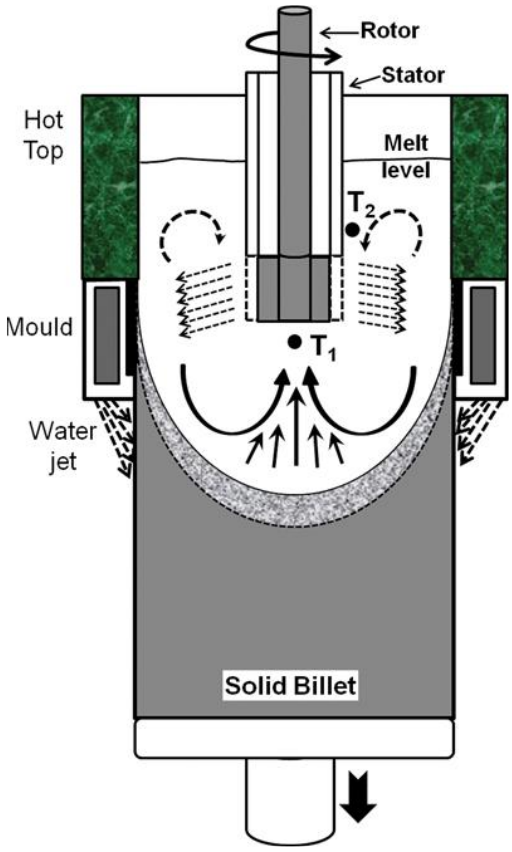

Figure 2.4: The schematic diagram illustrating the melt flow pattern in MC-DC casting process **[9]**.
Source: Prasada Rao (2014)

As demonstrated by (Prasada Rao, 2014), there were huge different between temperature T_1 and T_2 during the DC regime, as shown in **Figure 2.5 (a)**. In addition, the fluctuated of the huge temperature gradient during the DC regime was due to the irregularity of the heat and mass transfer in the billet sump. Nevertheless, the trend of

temperature T_2 changes dramatically during the transition from DC to MC-DC regime where, high shear device is switched ON, hence leads to isothermal regime. It is evident that the temperature drops just below the liquidus of the alloy, which is similar to the statement reported by (Xia et al., 2013) **[7,9]**. Therefore, the temperature at position T_1 and T_2 have achieved isothermal when come to MC-DC regime which also slightly below the temperature of liquidus as depicted in **Figure 2.5 (a, b)**.

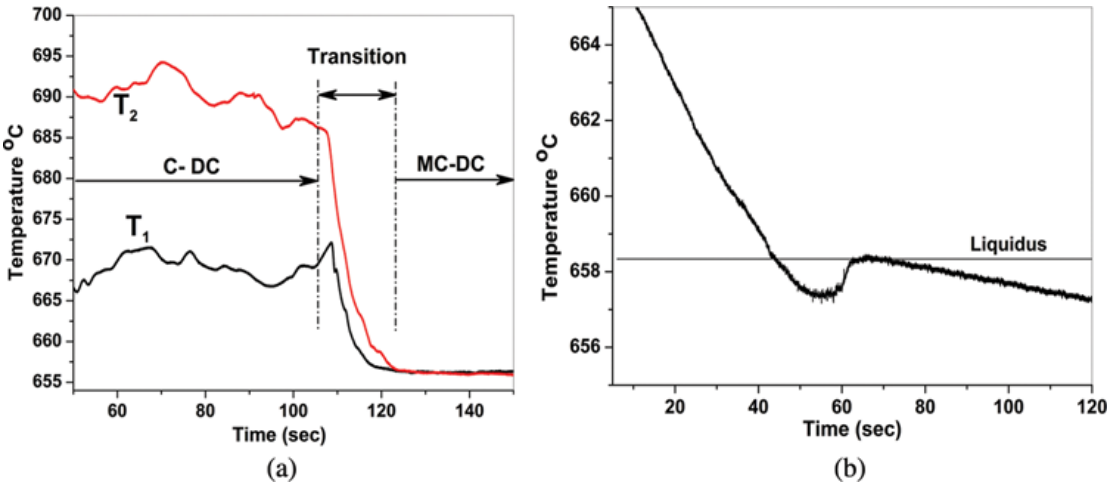

Figure 2.5: The temperature profiles of the (a) transition of sump temperature from DC to MC-DC casting and (b) typical cooling curve indicating the liquidus of the Al-6Zn alloy **[9]**.
Source: Prasada Rao (2014)

2.4 NUCLEATION IN DC CASTING OF LIGHT ALLOYS

(Fan et al., 2009) have reported that the macroscopic level of heterogeneous nucleation grow in melt conditioned DC casting is due to the high shear and high turbulence intensity of the fluid flow of molten melt. This phenomena has provided an extremely uniform distribution for both the temperature and chemical composition of the liquid melt throughout the entire cross section of the billets, hence the microstructural refinement happened when the created nuclei survive eventually. However, for the conventional process, most of the created nuclei in the first place tend to dissolve easily during the solidification process. Furthermore, the literature also reported the nucleation in microscopic level, the dispersed oxide particles due to high intensive force convection will potent heterogeneous nucleation **[4]**.

On the other hand, according to (M.C. Flemings, 1991), the fragmentation of dendritic particles that caused by severe forced convection, potent the nucleation growth for the solidification process **[21]**. Therefore, further research has been conducted for melt conditioning casting process to investigate the actual mechanism that responsible for the grain refinement in order to improve the cast quality of alloys.

In addition, (Xia et al., 2013) reported that , both nucleation and dendritic growth happen in the mushy zone under high shear forced convection throughout the melt. Interestingly, the floating rosettes formed in melt conditioned alloy is conceivable originated from the fragmentation of dendrite particles due to intensively shear force. In **Figure 2.6** stage-1, illustrated that the coarse dendrites is formed under DC process, where **Figure 2.6** stage-4, shown that the forced convection flow caused by the high shear has led to dendrites fragmentation and promote rosette growth **[10]**. Therefore, the solidification occurs in MC-DC casting by sedimentation of rosettes which then nucleation happens in the sump with isothermal temperature under forced convection flow **[7,10]**.

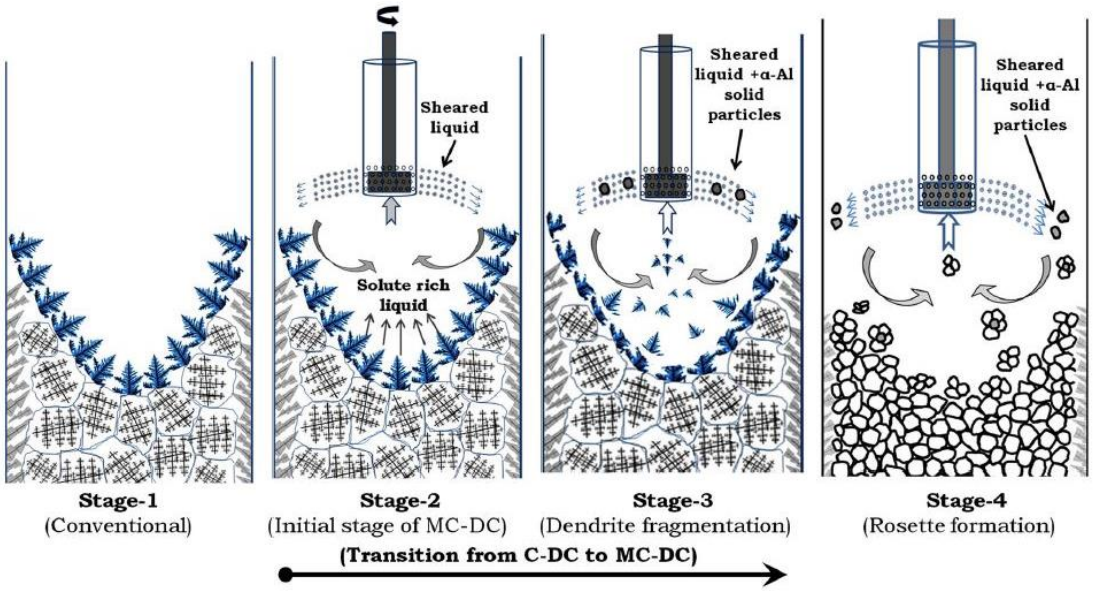

Figure 2.6: The schematic of the solidification transition from DC to MC-DC regime as the billet drops during casting **[10]**.
Source: Prasada Rao (2015)

Moreover, another promising result about the mechanism of heterogeneous nucleation in MC-DC casting was clearly reported by (Prasada Rao, 2015) **[10]**. In the past, the enhanced grain refinement in MC-DC cast billets was believed is due the

heterogeneous nucleation from the primary phase on the dispersed oxide particles by intensive melt shearing **[3-6]**. Unfortunately, the concept which stated by (M.C. Flemings, 1991) **[21]** on the nucleation which was cause by dendrite fragmentation was overlooked on the MC-DC casting process in the past work. In this paper, (Prasada Rao, 2015) **[10]** has well demonstrated the effect of dendrite fragmentation in MC-DC process under different casting speeds as shown in **Table 2.1**. Although the process is MCDC, but the grain refinement of the billets cast does not happen at extremely high casting speed. This is most probably due to the solid-liquid front of the billet cast remains un-ruptured by the high shearing rotor device under forced convention condition **[10]**. Therefore, the author has summarized the present work which confirmed that the mechanism is in well agreement with (M.C. Flemings, 1991) **[21]**. The evidence of the dendrites fragmentation has been illustrated in **Figure 2.7**, as a result the grain microstructure is refined under MC-DC regime throughout the billet cast **[9]**.

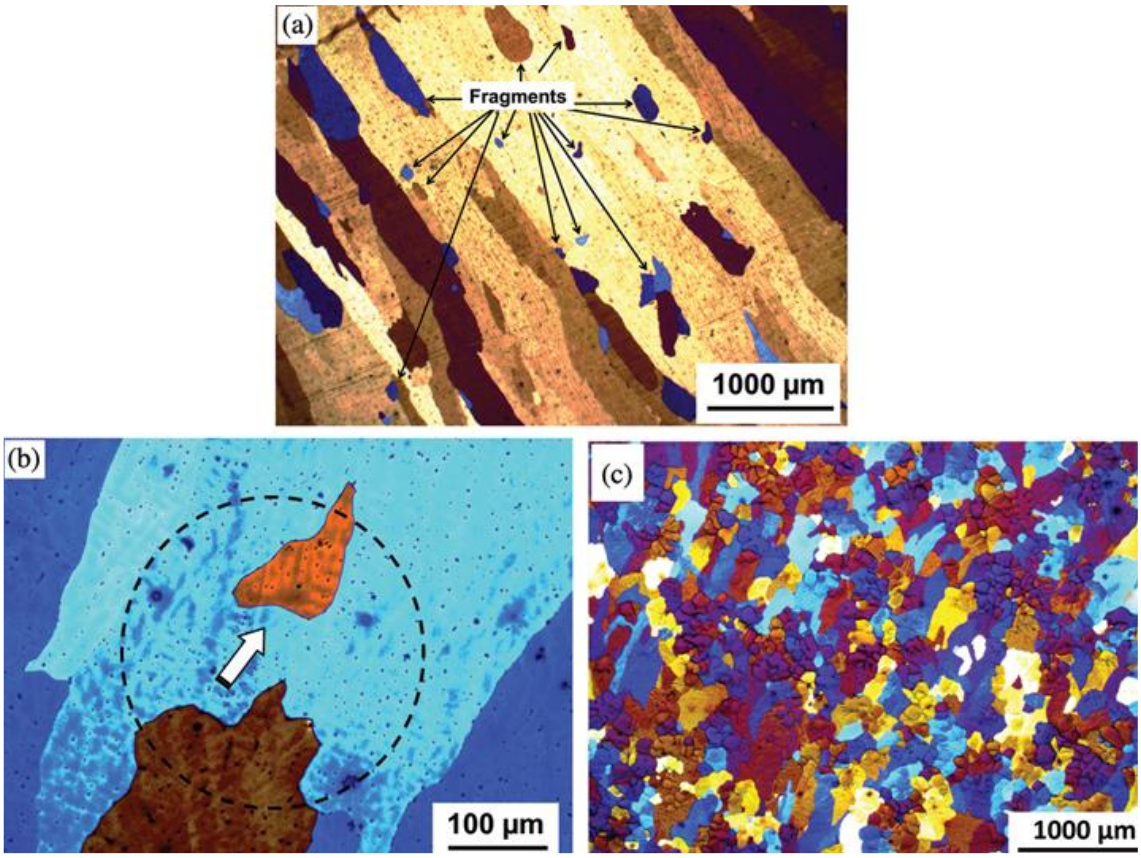

Figure 2.7: Optical photomicrographs of as-cast Al–6Zn alloy billet, corresponding to illustrating the dendrite fragmentation in MC-DC casting **[9]**.
Source: Prasada Rao (2014)

Table 2.1: The details of experiments of the CDC/MCDC casting process **[10]**.

Alloy	Grain refiner	Hold time, s	Billet casting speed, mm/min		Process	Grain size, μm	Billet #
			Start-speed	Steady state			
AA6xxx	...	20	140	200	CDC(a)	1103 ± 70	1
		20	140	200	MCDC	93 ± 10	2
		20	140	220	MCDC(a)	95 ± 12	3
	TiBAl	20	140	200	CDC	98 ± 14	4
LM6	...	25	240	240	CDC	995 ± 28	5
		25	280	280	MCDC	215 ± 12	6
Al-Fe (eutectic)	...	25	220	220	CDC	650 ± 18	7
		25	220	220	MCDC	260 ± 12	8
		25	300	300	CDC	980 ± 26	9
		25	300	300	MCDC	790 ± 18	10

Source: Prasada Rao (2015)

2.5 NUMERICAL MODELLING OF DC CASTING PROCESS

2.5.1 COMSOL Multiphysics

In this research, the software COMSOL Multiphysics is chosen as the solver for DC caster and MC-DC caster. COMSOL Multiphysics is a finite element analysis (FEA), solver and suitable for various physics and engineering application simulation. This FEA simulation software package which also suitable for research study and industrial scale application due to its flexibility study which enable user to integrate the interface environment designed for cross-disciplinary of product development, for example electrical, mechanical, heat transfer, fluid and chemical applications at once **[22]**.

An approach on industrial scale DC caster and MC-DC caster by using COMSOL Multiphysics software have been demonstrated by (Walinjkar & Rao, 2015). Walinjkar and Rao reported that the temperature gradient in the sump of MC-DC caster is reduced significantly when compare with the caster of DC. The simulation involved heat flow module and fluid flow module for both DC and MC-DC caster modelling, where for the MC-DC model the forced convection flow was chosen at the boundary of billet sump due to the stirring action from intense shearing device. Based on the research, it is interesting to know that the heterogeneous nucleation events occurs due to dendrite fragmentation in the isothermal region during the MC-DC casting process **[9,10]**. (Walinjkar & Rao, 2015) also successfully demonstrated that the attained

isothermal regime in the billet temperature sump profile was due to the high shearing device **[10,12]**.

2.5.2 Modelling of Direct Chill Caster

In the paper reported by (Sabau, Kuwana, Viswanathan, Saito, & Davis, 2004), by using ProCAST software, the heat transfer boundary conditions on the DC ingot must be applied on various surface of the ingot due to different heat transfer mechanism occur **[23]**. In another study by (Baserinia et al., 2012), the behaviour of the casting of Al-alloys in DC casting was modelled by using a commercial computational fluid dynamics (CFD) package ANSYS CFX. The DC modelling was solved with coupled heat transfer and fluid flow formulation for the 3D mould and water films, in order to estimate the coefficient of heat transfer **[24]**.

(H. Hu, Zhang, & Yang, 2008) also reported that the thermal stress contours and optimum casting parameters can be obtained from the solidifying of AZ31 DC casting billets via ANSYS software with FEA simulation **[25]**. Besides that, (W. Hu, Le, Zhang, Bao, & Cui, 2013) demonstrated the evolution of temperature in the AZ31 casting slab by DC casting process with different casting speed. The optimum casting parameters were chosen by comparing the temperature fields at various casting speed of slab by 3D numerical modelling **[26]**.

2.6 SUMMARY

Overall, this chapter had focused on the research on both DC and MC-DC casting process based on previous literature. The heat flow, casting parameters and the nucleation process of the cast billet from DC and MC-DC casting technique had well discussed with detailed description, figures and type of simulation from literatures with proper citations. Moreover, through this study, it was noted that the effect of the various parameters of the rotor-stator device has not been reported in the literature. Hence, it is interesting to analyse the effect of the shearing device parameters on the heat flow of cast billet and how it will determine the billet quality in present work.

CHAPTER 3

METHODOLOGY

3.1 INTRODUCTION

The methodology of this research project involves simulation of both DC and MC-DC casting of AZ31 Mg-alloy using COMSOL Multiphysics 4.4 through FEA mesh analysis. Basically, the 3D models of a conventional direct chill (DC) caster and a melt conditioned direct chill (MC-DC) caster with rotor-stator based shearing device were created by using COMSOL Multiphysics software. The casts of AZ31 Mg-alloy billets with the solidification range (80 ℃) were simulated by using the modules of heat flow and fluid flow in COMSOL Multiphysics. Therefore, the present research has been focused on understanding the evolution of temperature sump profile distribution in an industrial scale of cast billet with a diameter of 206 mm and a length of 7000 mm for both DC and MC-DC casting process. The various rotor-stator parameters were manipulated in the case of MC-DC, in order to study the heat flow.

In addition, the effect of the depth of rotor-stator and the rotor-stator diameter have been modelled to investigate the evolution of temperature distribution. The process flow has been explained in **Figure 3.1**, which illustrates the flow of the project methodology. The time line of the research has been provided in **Appendix A**, which demonstrates the Gantt charts of the overall project.

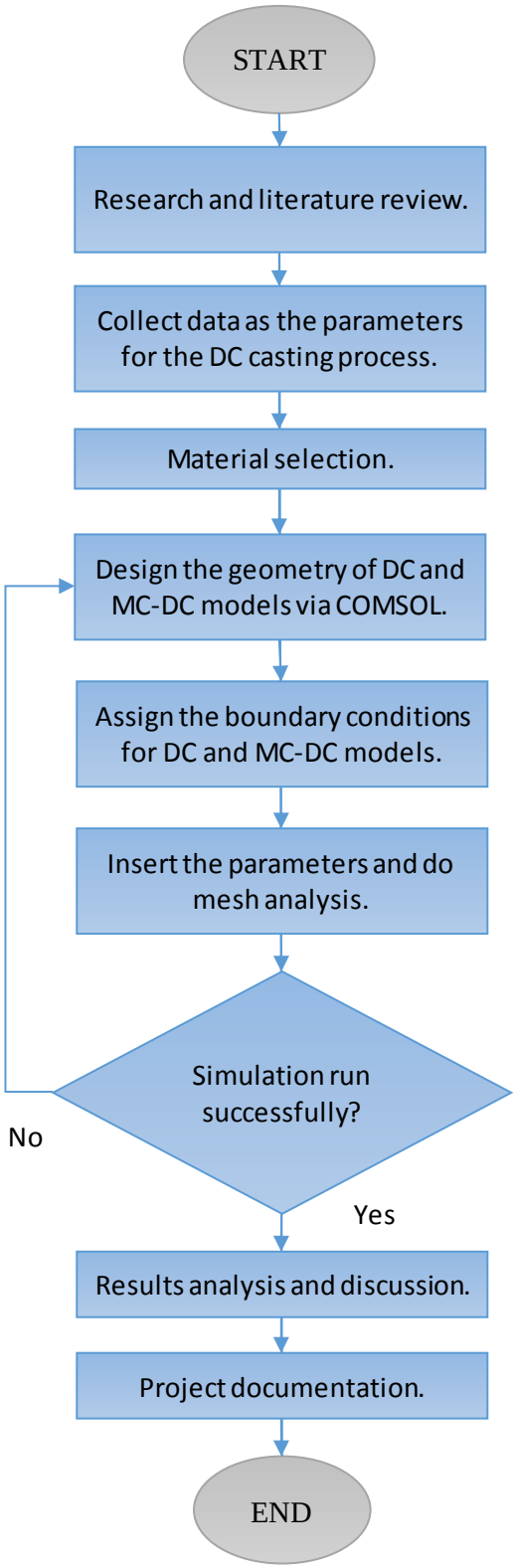

Figure 3.1: Flowchart of methodology.

3.2 METHODOLOGY

The framework of this project has been depicted in **Figure 3.2**. First of all, the geometry of the caster for both DC and MC-DC with rotor-stator based high shearing device were created by using COMSOL Multiphysics software. Then the AZ31 Mg-alloy was chosen as the material of the cast billet in this research study.

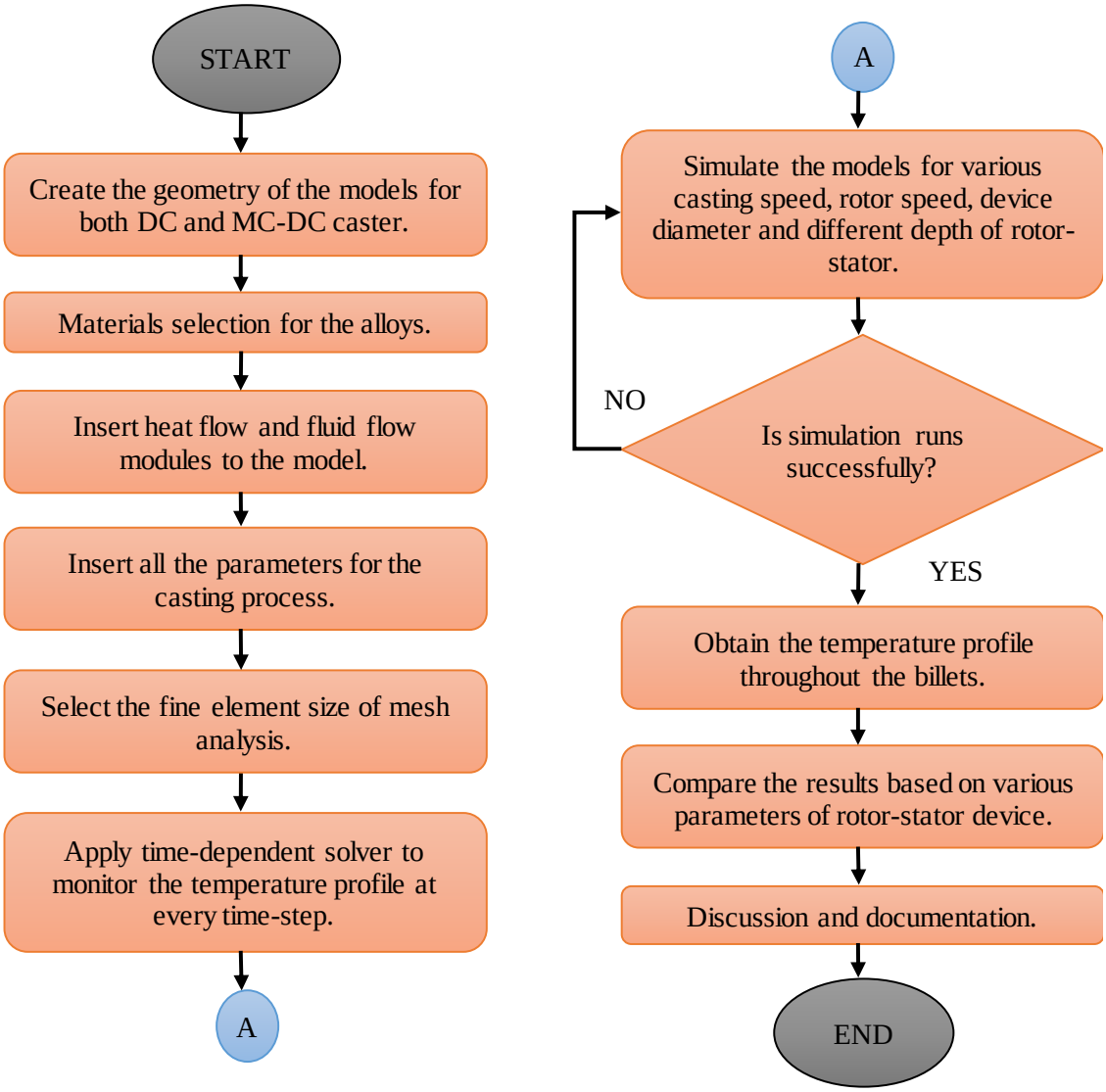

Figure 3.2: Flowchart of Simulation Process.

Furthermore, the physics of heat flow and fluid flow modules were added to the specified boundaries with specified conditions. Then, the parameters such as casting speed, water flow rate and rotor speed were decided later. In order to obtain a good result, the fine mesh analysis was applied to the DC and MC-DC models. After that, the time dependent solver in COMSOL was used to monitor the evolution of temperature sump profile distribution at every time step of heat flow in the DC and MC-DC models cast billets. Additionally, the rotor speed was varied with different depths of immersion and different rotor diameter of the shearing device during the MC-DC casting process. The obtained results were further compared and analysed in order to investigate the optimum parameters.

3.3 GEOMETRY DESIGN

In the present work, the DC and MC-DC cast billets were designed according to the industrial scale billet size (diameter of 206 mm; length of 7000mm). The cast billets were developed in 2D axis symmetrical with the heat transfer module and fluid flow module. Further engineering assumptions and boundary conditions of the DC and MC-DC cast billets in COMSOL Multiphysics have been demonstrated.

3.3.1 Geometry of DC Caster

In **Figure 3.3** illustrated the geometry of DC caster was designed by COMSOL Multiphysics based on the industrial scale of the billet with the dimension of 206 mm (0.206 m) in diameter and 7000 mm (7 m) in length. The detail dimension of the DC caster was provided in **Table 3.1**, where the whole cast billet and graphite lining were constructed by using rectangles and, the wagstaff mould (aluminium mould) with water container were created by using polygon lines. Moreover, in **Table 3.2** illustrated the statistics for the number of domains and the number of boundaries between each domain in the DC geometry.

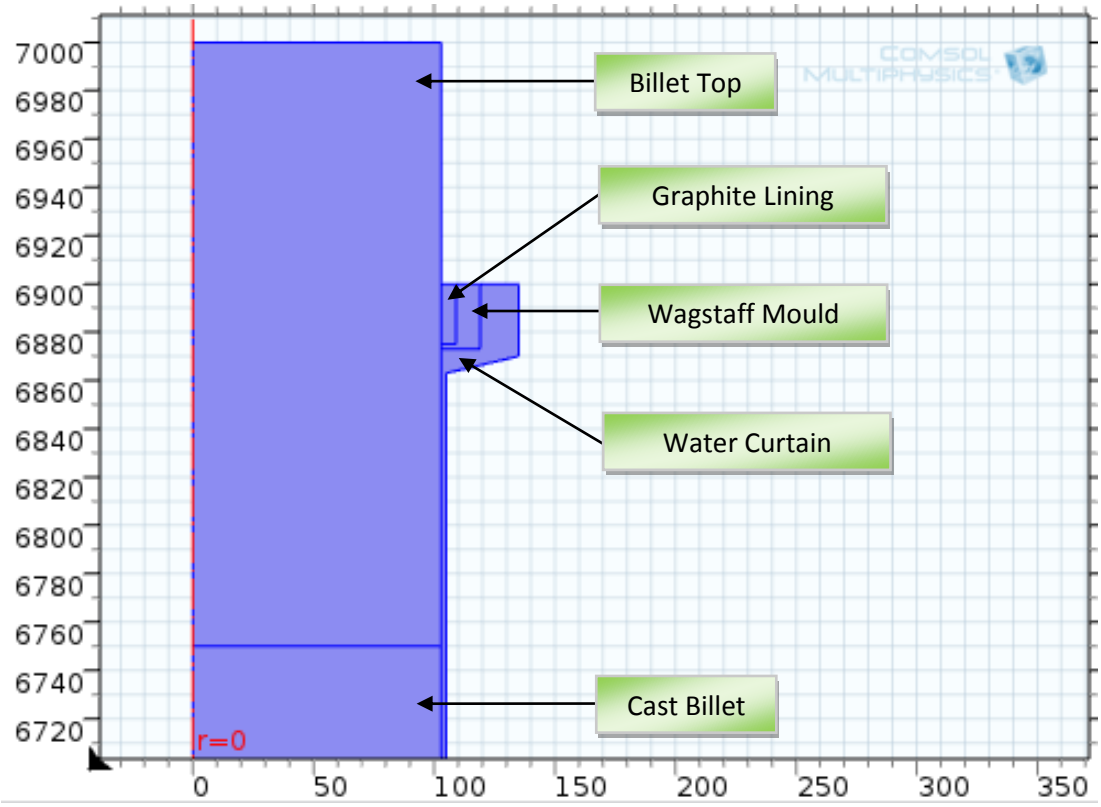

Figure 3.3: Geometry of DC caster in 2D axis symmetry.

Table 3.1: Dimensions of Direct Chill Caster in COMSOL Multiphysics.

Name	Dimension (mm)
Billet Top	{{0, 6750}, {103, 6750}, {103, 7000}, {0, 7000}, {0, 6750}}
Cast Billet	{103, 7000}
Graphite Lining	{6, 25}
Wagstaff Mould	{{103, 6875}, {109, 6875}, {109, 6900}, {119, 6900}, {119, 6873}, {103, 6873}, {103, 6875}}
Water Curtains	{{103, 6873}, {119, 6873}, {119, 6900}, {135, 6900}, {135, 6870}, {105, 6863}, {105, 0}, {103, 0}, {103, 6873}}

Table 3.2: Geometry Statistics of Direct Chill Caster.

Property	Value
Space dimension	2
Number of domains	5
Number of boundaries	21
Number of vertices	17

3.3.2 Geometry of MC-DC Caster

In **Figure 3.4** illustrated the 2D axis symmetry of MC-DC caster which was designed by COMSOL Multiphysics based on the industrial scale of the billet with the dimension of 206 mm (0.206 m) in diameter and 7000 mm (7 m) in length. Moreover, the MC-DC caster was acquired with the rotor-stator shearing device in the diameter of 80mm. The rotor-stator device was immersed in the billet top of the caster. The detail dimension of the MC-DC caster was provided in **Table 3.3**, where the whole billet and graphite lining were constructed by using rectangles and, the shearing device, wagstaff mould or aluminium mould and water curtain were created by using polygon lines by specifying the data points as in **Table 3.3**. Moreover, in **Table 3.4**, illustrated the statistics for the number of domains and the number of boundaries between each domain in the MC-DC geometry.

Furthermore, proceeding to the materials selection and physics module study by using COMSOL Multiphysics. Both heat flow and fluid flow module were used in an attempt to simulate for the Mg-alloy cast billet within the solidification range of 80 ℃. The parameters for the simulation were manipulated with previous studies. For inlet of the liquid metal was considered to be 690 ℃ (963.15 K) with the casting speed of 300 mm/min (0.005 m/s). Additionally, the inlet water was at the temperature of 10 ℃ (283.15 K) with a fluid flow velocity of 0.5 m/sec along the billet surface during the casting process.

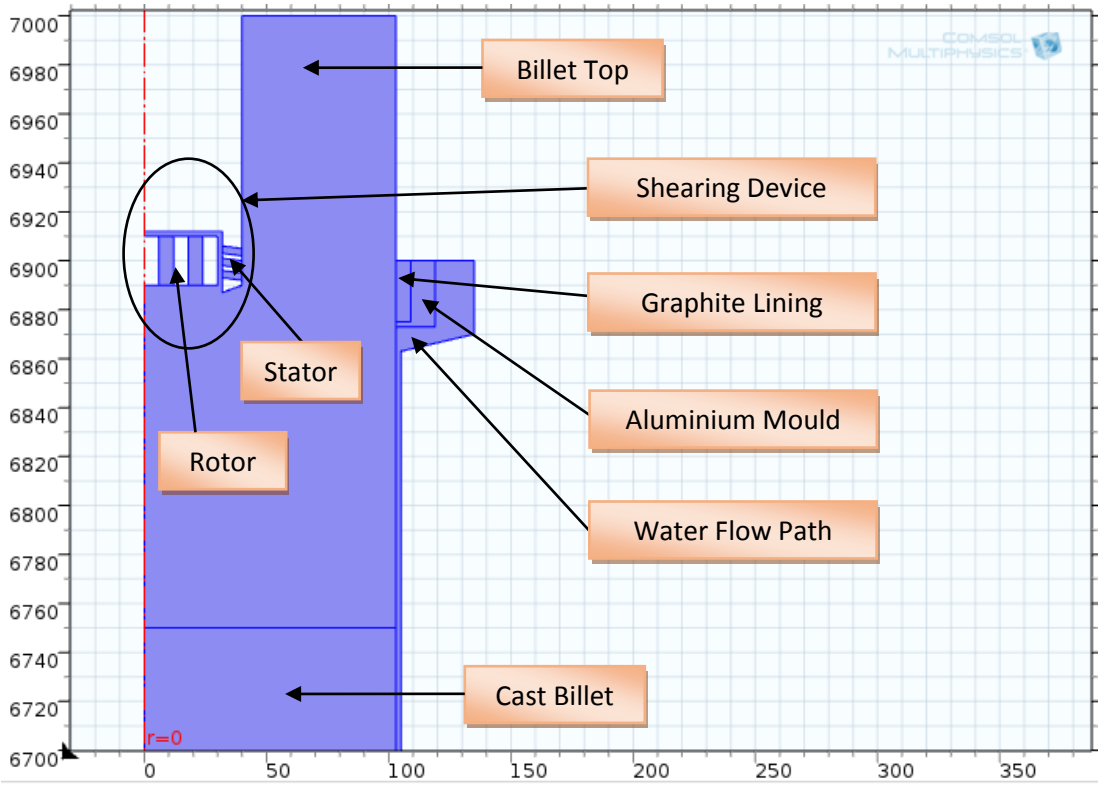

Figure 3.4: Geometry of MC-DC caster in 2D axis symmetry.

Table 3.3: Dimensions of MC-DC Caster in COMSOL Multiphysics.

Name	Dimension (mm)
Billet Top with Shearing Device	{{0, 6800}, {103, 6800}, {103, 7000}, {40, 7000}, {40, 6907}, {0, 6907}, {40, 6907}, {40, 6895}, {39.5, 6895}, {39.5, 6907}, {0, 6907}, {0, 6905}, {38, 6905}, {38, 6895}, {0, 6895}, {0, 6800}}
Rotor	{{6, 6910}, {6, 6890}, {12, 6890}, {12, 6910}, {18, 6910}, {18, 6890}, {24, 6890}, {24, 6910}}
Stator	{{32, 6893}, {40, 6892}, {40, 6895}, {32, 6896}, {32, 6898}, {40, 6897}, {40, 6900}, {32, 6901}, {32, 6903}, {40, 6902}, {40, 6905}, {32, 6906}}
Cast Billet	{103, 7000}
Graphite Lining	{6, 25}
Wagstaff Mould	{{103, 6875}, {109, 6875}, {109, 6900}, {119, 6900}, {119, 6873}, {103, 6873}, {103, 6875}}
Water Curtains	{{103, 6873}, {119, 6873}, {119, 6900}, {135, 6900}, {135, 6870}, {105, 6863}, {105, 0}, {103, 0}, {103, 6873}}

Table 3.4: Geometry Statistics of MC-DC Caster.

Property	Value
Space dimension	2
Number of domains	10
Number of boundaries	59
Number of vertices	45

3.4 MATERIALS SELECTION IN SIMULATION

In this simulation, the material of the cast billet was filled with molten liquid of Magnesium alloys, namely AZ31 Mg-alloys. The thermo-physical properties of AZ31 alloy ware specified throughout the experiment for both DC and MC-DC simulations **[25, 26, and 28]**. There was a heat transfer with phase transformation for the AZ31 from superheated liquid state to solid state, hence, in **Table 3.5** and **Table 3.6**, illustrated the parameters of AZ31 for as liquidus and solidus respectively in COMSOL Multiphysics.

Table 3.5: Parameters of AZ31 (UNS M11311) [liquid] at liquidus.

Name	Value	Unit
Heat capacity at constant pressure	C_liquid_2(T[1/K])[J/(kg*K)]	J/(kg*K)
Thermal conductivity	60	W/(m*K)
Density	1000	kg/m^3
Ratio of specific heats	1	1
Dynamic viscosity	0.001	Pa*s

Table 3.6: Parameters of AZ31 (UNS M11311) [solid] at solidus.

Name	Value	Unit
Thermal conductivity	k(T[1/K])[W/(m*K)]	W/(m*K)
Heat capacity at constant pressure	C_solid_1(T[1/K])[J/(kg*K)]	J/(kg*K)
Density	rho(T[1/K])[kg/m^3]	kg/m^3
Ratio of specific heats	1	1

Besides that, the water curtains was filled with H_2O, also called water. In the simulation, there was heat transfer with phase transformation from water to vapour. Therefore, the considerate parameters for both liquid state and gas state were shown in **Table 3.7** and **Table 3.8** respectively in COMSOL Multiphysics.

Table 3.7: Parameters of H_2O (water) [liquid].

Name	Value	Unit
Thermal conductivity	k_liquid_2(T[1/K])[W/(m*K)]	W/(m*K)
Heat capacity at constant pressure	C_liquid_2(T[1/K])[J/(kg*K)]	J/(kg*K)
Density	rho_liquid_2(T[1/K])[kg/m^3]	kg/m^3
Dynamic viscosity	eta_liquid_1(T[1/K])[Pa*s]	Pa*s
Ratio of specific heats	1	1

Table 3.8: Parameters of H_2O (water) [gas].

Name	Value	Unit
Thermal conductivity	k_gas_3(T[1/K])[W/(m*K)]	W/(m*K)
Heat capacity at constant pressure	C_gas_3(T[1/K])[J/(kg*K)]	J/(kg*K)
Density	958	kg/m^3
Ratio of specific heats	1.33	1

Moreover, the material of the wagstaff mould was built with the material of aluminium alloy 6070 solid and the graphite lining was the Pyrolytic graphite in solid state. Both of the parameters were shown in **Table 3.9** and **Table 3.10** respectively as in COMSOL Simulation as well.

Table 3.9: Parameters of 6070 (UNS A96070) [solid].

Name	Value	Unit
Density	rho(T[1/K])[kg/m^3]	kg/m^3
Thermal conductivity	171	W/(m*K)
Heat capacity at constant pressure	891	J/(kg*K)

Table 3.10: Parameters of Pyrolytic Graphite [solid, annealed].

Name	Value	Unit
Heat capacity at constant pressure	C_solid_annealed_2(T[1/K])[J/(kg*K)]	J/(kg*K)
Density	rho(T[1/K])[kg/m^3]	kg/m^3
Thermal conductivity	70	W/(m*K)

3.5 CONDITIONS OF DC AND MC-DC CASTING

The initial conditions of the pouring temperature, preheated shearing device and hot top were confirmed and setup for both DC caster and MC-DC caster as shown in **Table 3.11**.

Table 3.11: Initial Condition of the DC and MC-DC caster at assumed room temperature of 20 ℃.

Description	Value
Inlet temperature of the liquid metal	690 ℃ (963.15 K)
Initial temperature of shearing device	690 ℃ (963.15 K)
Initial temperature of hot top	690 ℃ (963.15 K)
Initial temperature for wagstaff mould	10 ℃ (283.15 K)
Initial temperature for graphite lining	10 ℃ (283.15 K)
Inlet temperature of water	10 ℃ (283.15 K)

Temperature Strain Reference of Mg-alloy (AZ31)

- Liquidus at: 630 ℃ (903.15 K).
- Solidus at: 550 ℃ (823.15 K).
- Solidification Range = 80 ℃.

Velocity of the system

- Water flow rate: 0.5 m/sec.
- Casting speed: 300 mm/min (0.005 m/sec)
- Rotor-stator shearing speed: 0 rpm, 50 rpm, 100 rpm, 200 rpm, and 300 rpm.

3.5.1 Simulation of DC Casting

In this section, a DC caster with 300 mm/min (0.005 m/s) of casting speed has been modelled in order to obtain the temperature profile of the simulation and analysed the depth of the sump of the billet. In order to obtain an accurate results, the fine element size of mesh analysis was selected to analyse the billet with the heat transfer module and the fluid flow module as shown in **Figure 3.5**.

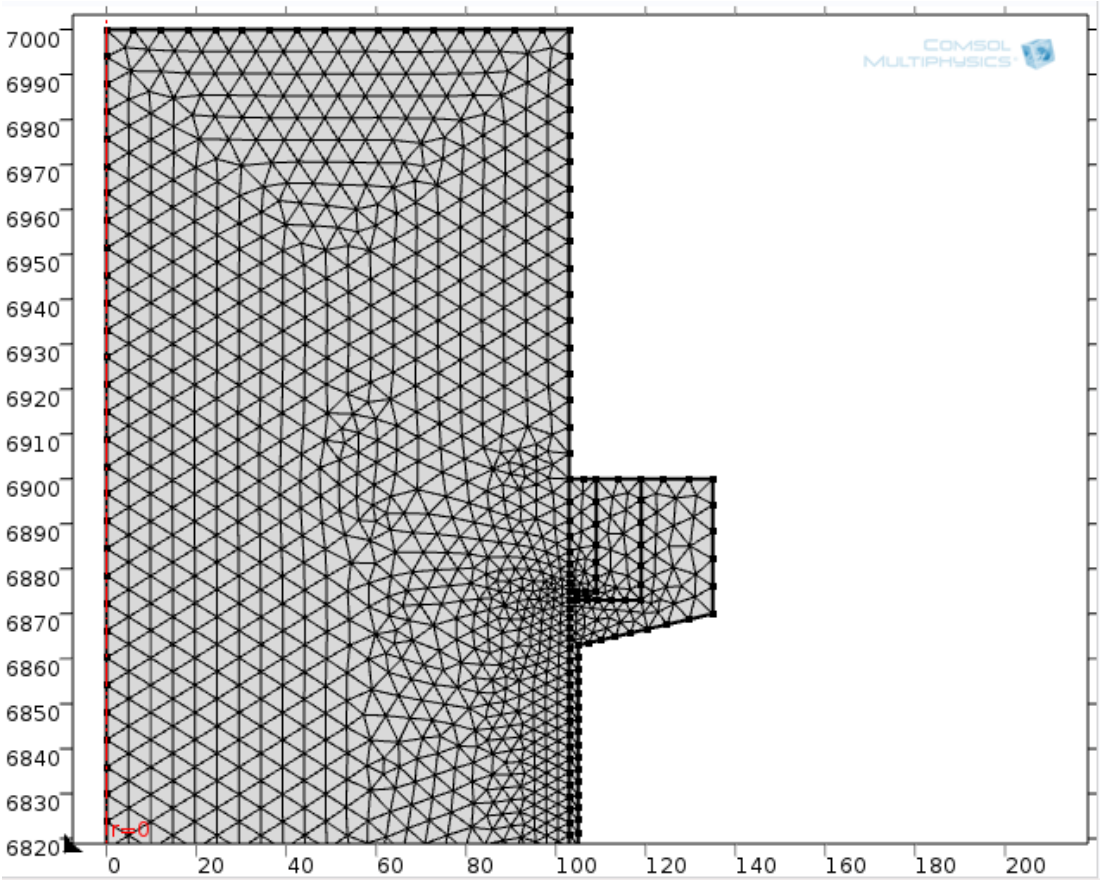

Figure 3.5: Fine element size of mesh analysis in DC caster.

3.5.2 Boundary Conditions of DC Casting

The boundary condition for heat transfer and fluid flow modules have been divided into two major parts which were the primary cooling zone and secondary cooling zone. At primary cooling zones, the boundaries condition were focused on the water cooled mould which included the graphite lining and aluminium mould. Where the secondary cooling zones involved the boundaries between water films that directly

contact on the billets surface **[11]**. First of all, there was thermal insulation for the hot top of the caster. During the DC casting process, the hot top was preheated to the temperature of 690 ℃ (963.15 K), hence, there was no heat loss from the billet top, since, the initial temperature of the hot top caster was in isothermal with the pouring temperature **[9,10,25,28]**. In **Figure 3.6**, depicted the boundary as blue labelled lines were in thermal insulated condition. Whereas, for the cast inlet boundary was set to be 690 ℃ (963.15 K), due to the superheated molten melt is going to pour into the caster with an uniform inlet velocity was applied **[27,33,38]**.

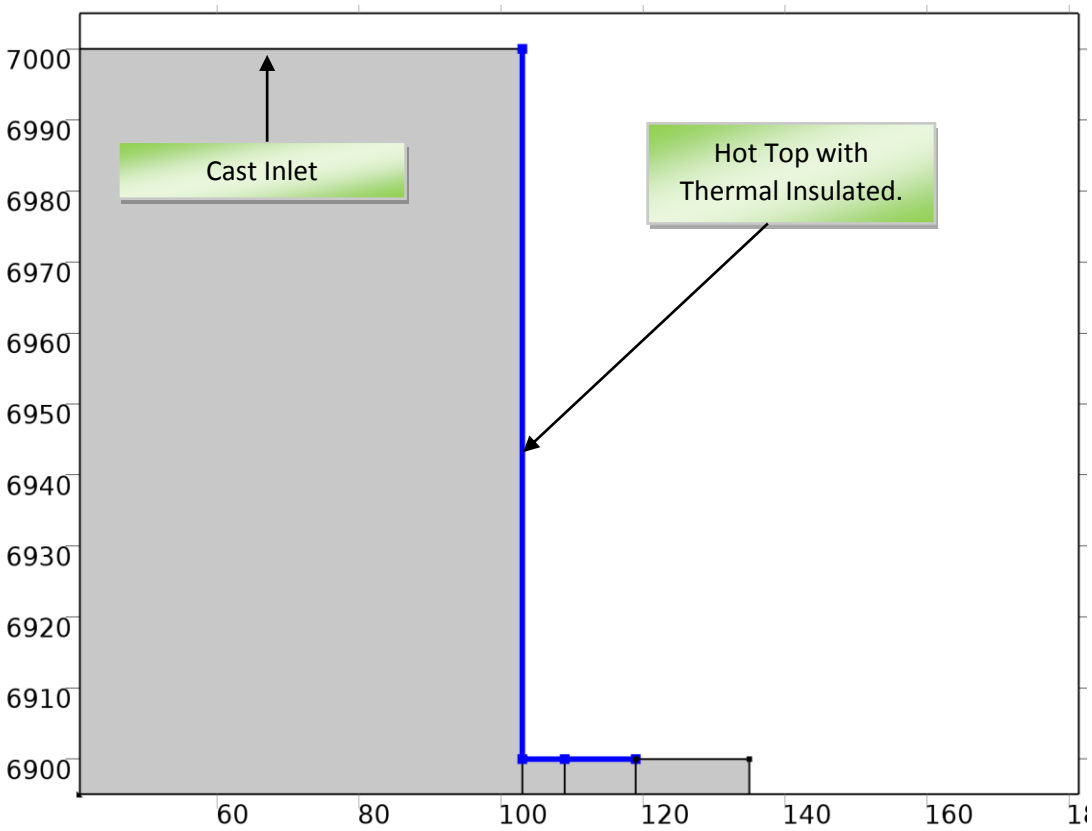

Figure 3.6: Thermal Insulation of DC caster.

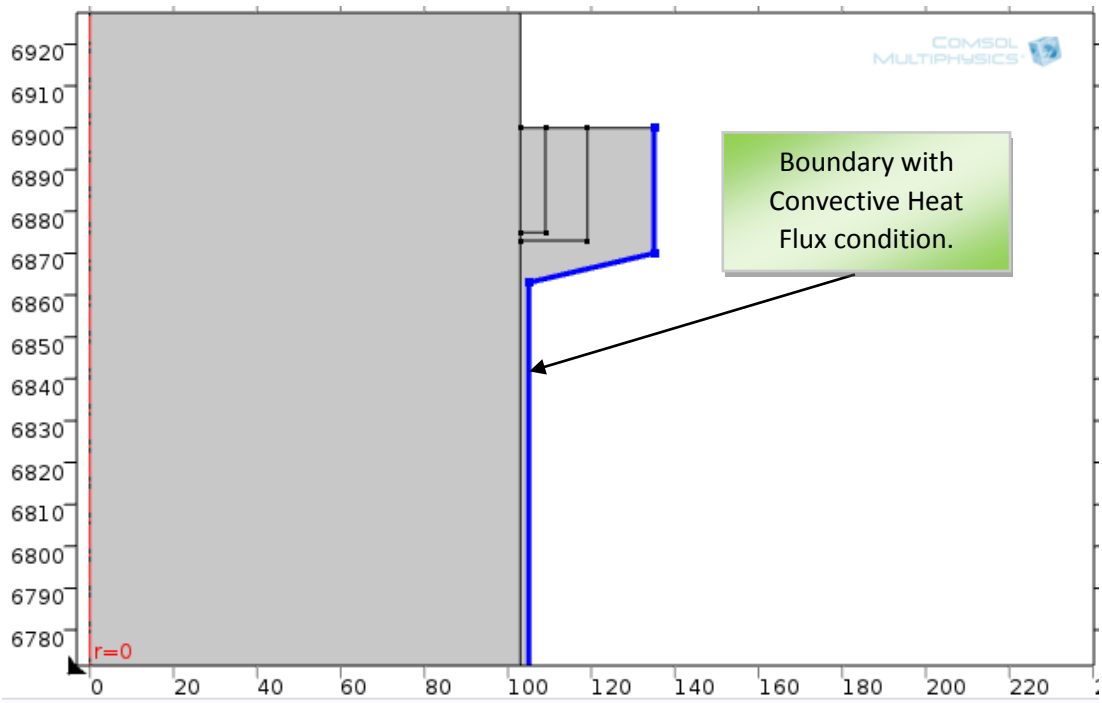

Figure 3.7: Convective Heat Flux of DC caster.

There was an unavoidable of convective heat flux between the cooled water film and external environment for the boundary as blue labelled in **Figure 3.7**. This phenomena happened due to the high temperature gradient between the water and surface of cast billet that lead to the evaporation of cooled water to the external environment **[23]**. There was a heat transfer with phase transformation of the cooled water liquid to vapour gases during the casting process due to the cold water was heated up to its boiling point of 100 ℃ (373.15 K) as shown in **Table 3.12**. Besides that, there were also a heat transfer in solids between the cast billet to the solid graphite lining and solid aluminium mould as well.

During the casting process, the molten liquid begins to solidify when its first contact with the graphite and aluminium mould, thereby, the first solid shell was formed and hold by a starter block with specific casting speed. Then, the molten melts was fed continuously and allow the direct chill water spray on its shell to extract the heat. Therefore, the huge temperature gradient has led to phase transformation of AZ31 from liquid to solid in the caster **[27]**. **Table 3.13** shows the phase transformation of the AZ31 with referred to the liquidus temperature of 630 ℃ (903.15 K) and solidus temperature of 550 ℃ (823.15 K) for the Mg alloys.

During the laminar flow of the casting process, there was a slip condition along the wall of cast billet with the wall of hot top, graphite lining, aluminium mould and impingement zone of water to allow the cast billet to free slip with the specify casting speed. The same condition applies to the water films at the secondary cooling zone, which allow water to slip through the billet surface according to its water flow rate. A slippery condition was required to protect the inner wall of the aluminium mould at pre-casting stage and to prevent the solidified metal sticking on the mould **[11, 25, 26, 34, and 36]**. The slip condition was as depicted as blue labelled in **Figure 3.8**. Furthermore, there was a condition for the domain of graphite lining and aluminium mould which was heat transfer between solids as shown in **Figure 3.9**.

Table 3.12: Parameters of Phase Transformation of H_2O.

Description	Value
Phase change temperature between liquid phase and gas phase	373.15[K]
Transition interval between liquid phase and gas phase	100[K]
Latent heat from liquid phase and gas phase	2257[kJ/kg]

Table 3.13: Parameters of Phase Transformation of AZ31.

Description	Value
Phase change temperature between liquid phase and solid phase	903.15[K]
Transition interval between liquid phase and solid phase	80[K]
Latent heat from liquid phase and solid phase	368[kJ/kg]

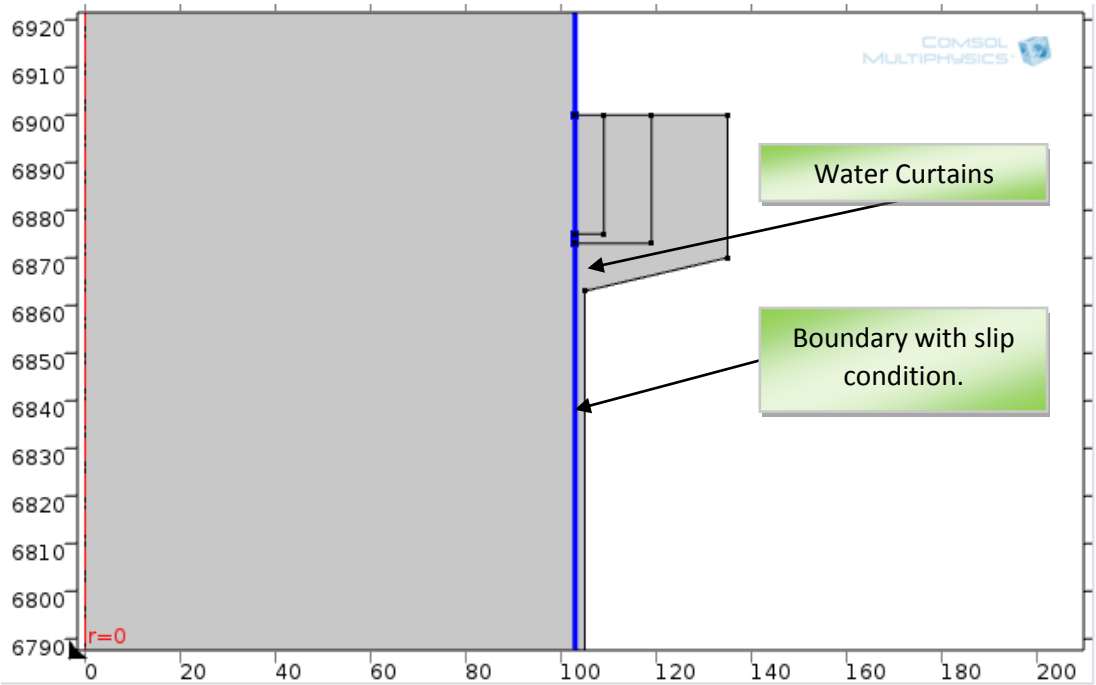

Figure 3.8: Boundary with Slip Condition of DC caster.

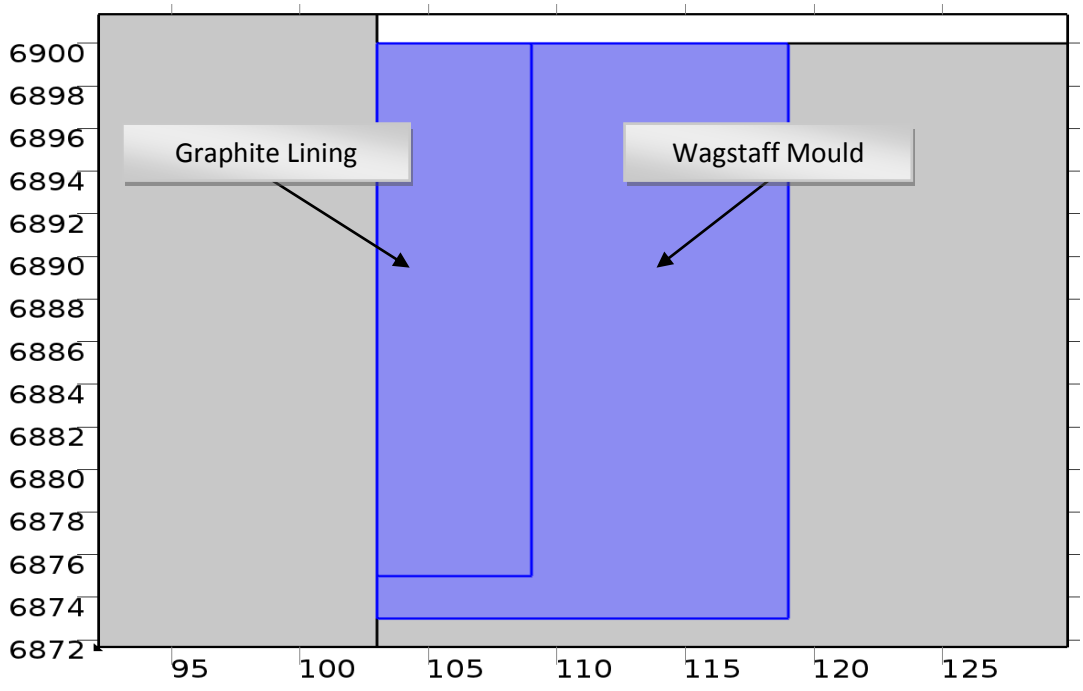

Figure 3.9: Heat Transfer between graphite lining and aluminium mould.

3.5.3 Simulation of MC-DC Casting

With the casting speed of 300 mm/min, the DC was modelled with the integration of rotor-stator device, hereby termed as MC-DC casting process. In this approach, five simulations for the MC-DC caster were conducted with various rotor speed, that were 0 rpm, 50 rpm, 100 rpm, 200 rpm, and 300 rpm. The fine element size of mesh analysis was applied to whole domains of MC-DC billet, caster and the shearing device as shown in **Figure 3.10**.

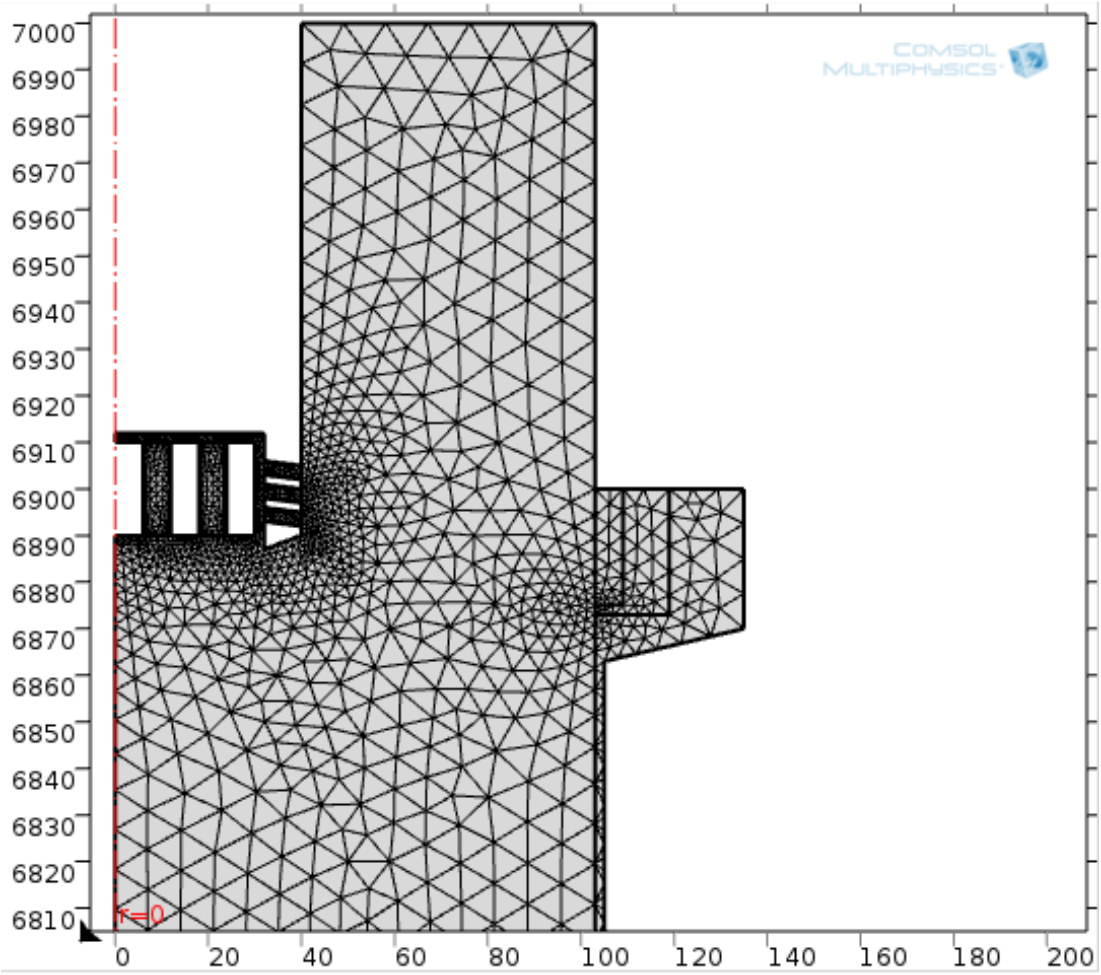

Figure 3.10: Fine element size of mesh analysis in MC-DC caster.

3.5.4 Boundary Conditions of MC-DC Casting

In MC-DC simulation, the boundary conditions were maintained as same as the DC caster, just with an addition of rotor-stator shearing device immersed in the billet top. Forced convection flow was generated by rotor-stator upon the MC-DC billet sump during the casting process **[12]**. Therefore, only the boundary conditions for rotor-stator shearing device were discussed in this section.

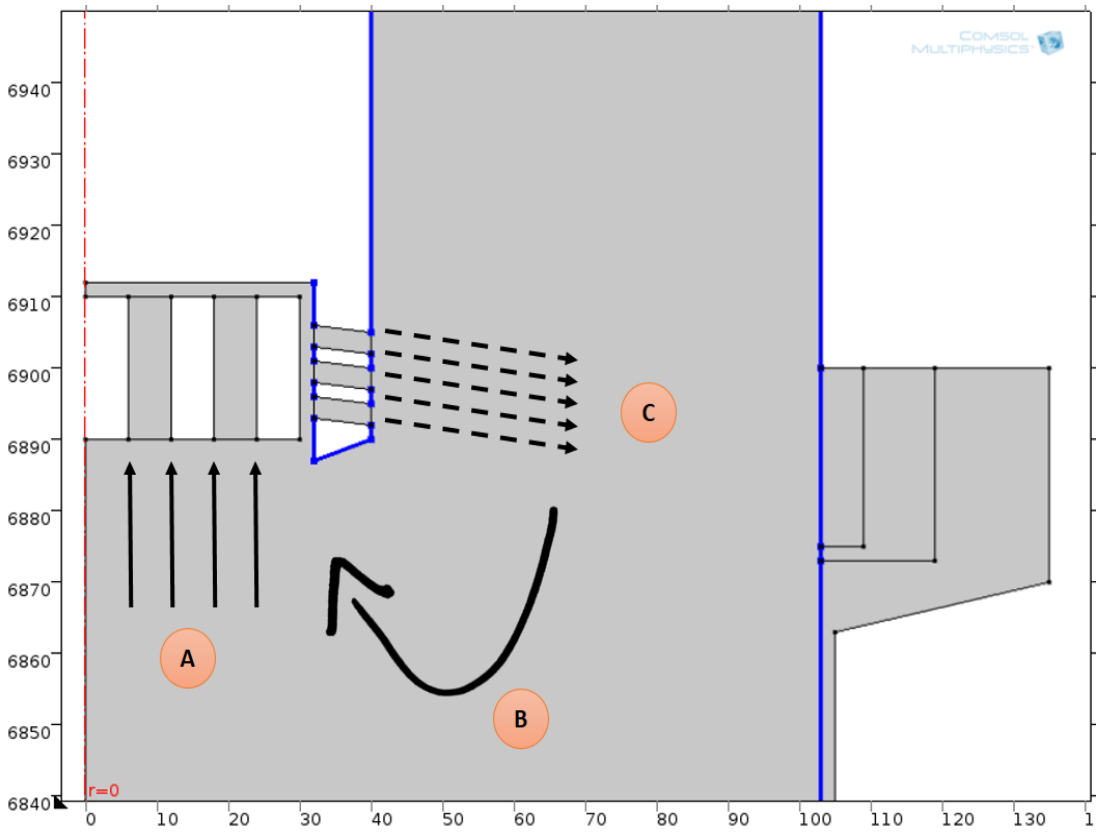

Figure 3.11: Forced Convection flow pattern in billet top of MC-DC caster.

In the billet top of the caster, the AZ31 molten liquid was allowed to pour in the caster from the inlet surrounded by hot top. The device was assumed in the same temperature to hot top, 690 ℃ (963.15 K), since it required to preheated prior to casting process **[9,10]**. The free-slip condition was applied to the inner wall of mould and the outer surface of the stator cage as indicated as blue labelled line in **Figure 3.11**. The casting speed allowed the billet to eject vertically downwards. As the rotor was turned "ON", the liquid changes its flow-path as indicated by arrows A, B and C sequentially as shown in the **Figure 3.11**.

Furthermore, the wall conditions for the rotor-stator shearing device was allowed to rotate in radial flow with the speed of 0 rpm, 50 rpm, 100 rpm, 200 rpm and 300 rpm. The shearing device considered in this work is a flat blade turbine mixer that generates the radial flow or forced convection in the billet sump with intensive shearing rate **[29-32]**.

For more information, the MC-DC casting process is actually an agitation process of fluid mixing in the billet sump. In such situations, a radial flow impeller such as rotor-stator type shearing device is utilized to achieve the intensive shearing rate during the dispersion process **[29-32]**.

3.6 MODELLING ASSUMPTIONS

In addition, the engineering assumptions of the model are to be discussed. For both DC and MC-DC caster, a 2D axis symmetry was assumed to reduce the heat flow problem into two directions namely radial and axial. Furthermore, the centreline of the billets was assumed to have without heat loss due to the symmetry **[11, 35, 36, and 38]**. The liquid flow was considered laminar according to the velocity and inlet dimensions. The material AZ31 magnesium alloy was considered as a phase transformation mixture between liquid and solid. Besides that, the fluid was assumed to behave as an incompressible Newtonian fluid, where the thermoplastics properties were specifically obtained based on the materials respectively **[33, 39]**.

CHAPTER 4

RESULTS AND DISCUSSIONS

4.1 INTRODUCTION

In this work, four different cases of study have been discussed and demonstrated. The relative parameters that involved in this study was shown in **Table 4.1**. Results have been obtained by various parameters such as casting speed, rotor speed, depth of rotor-stator device and diameter of rotor-stator device. The results temperature sump profiles were recorded in the COMSOL Multiphysics software. These parameters were reported to show a significant effect on the bleed-outs and hot-tears during the billet casting process.

Table 4.1: The Various Parameters Involved in this Study.

No.	Parameter	Value	Unit
1.	Casting Speed.	100, 300, and 500.	mm/min
2.	Rotor Speed.	0, 50, 100, 200, and 300.	rpm
3.	Depth of rotor-stator device from the hot top.	100 and 110.	mm
4.	Diameter of rotor-stator device.	40 and 80.	mm

4.2 SIMULATION RESULTS AND DISCUSSIONS

Simulated results have been shown respectively according to the study, and the results shall demonstrate the effect of the various casting speed on the temperature sump profile, effect of rotor speed on the temperature sump profile, effect of device depth on the temperature sump profile and the effect of device depth on the temperature sump profiles.

4.2.1 Simulation of Conventional DC Casting

A conventional type of casting, direct chill casting has been simulated in order to demonstrate the differences in various parameters later on. An industrial scale of a casting billet with the diameter of 206 mm; length of 7000 mm has been modelled in the COMSOL environment at 100 mm/min, 300 mm/min and 500 mm/min of casting speed. Some influence of the parameters on the possible defects has been discussed.

Based on the results as illustrated in **Figure 4.1, 4.2 and 4.3**, three different cases have been shown. In **Figure 4.1** shows the steady state of DC cast billet sump profile corresponding to casting speed of 100 mm/min. In low casting speed, the depth of the sump is shallower and have thicker shell wall. As the casting speed increases to 300 mm/min as in **Figure 4.2**, the sump profile exhibited a deeper depth of the sump with thinner shell wall compared to the former as illustrated in **Figure 4.1**. For the highest casting speed among three, 500 mm/min of casting speed was simulated, with the result presented in **Figure 4.3**. The results have revealed that as the casting speed increase, the deeper the depth of sump and the thinner is the shell wall **[39]**.

In addition, some literature has discussed that the higher the casting speed may improve the production time and more productivity, meanwhile, the higher casting speed able to minimize the cold-shuts effect. As the casting speed increase, the shell thickness becomes thinner. This has led to the increasing depth of billet sump and causing defects such as bleed-outs. Literature also reported at a higher casting speed, uneven solute distribution occurred in the billet sump, hence led to hot-tears and irregular porosity **[18]**. In other words, at higher casting speed, the solid at primary shell spends less time for heat extraction and primary cooling compared with the lower casting speed model. Although, the improvement of the productivity is necessary by increasing the casting speed. However, the defects such as porosity, hot-tears and bleed-outs have to be solved as casting speed increases **[9-11, 37, 38]**.

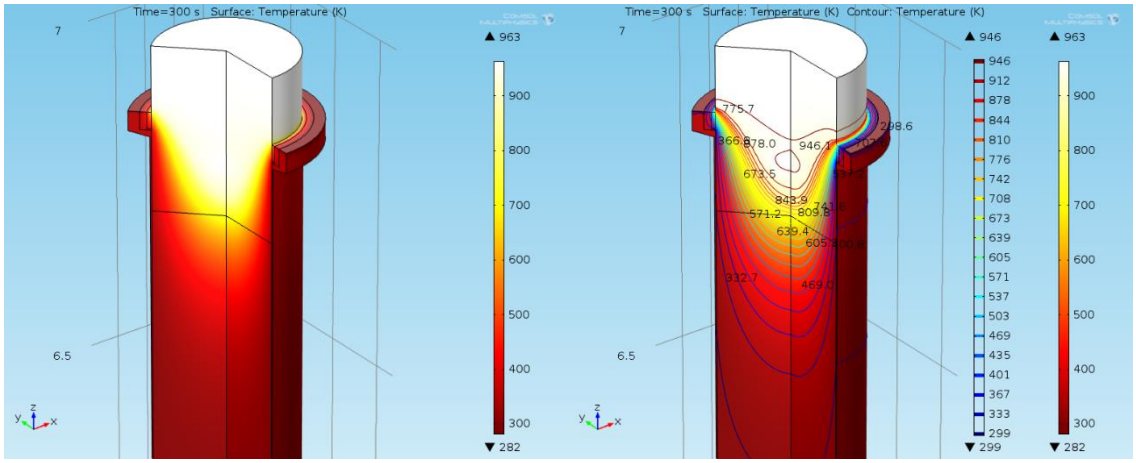

Figure 4.1: Steady state of DC cast billet sump profile corresponding to casting speed of 100 mm/min.

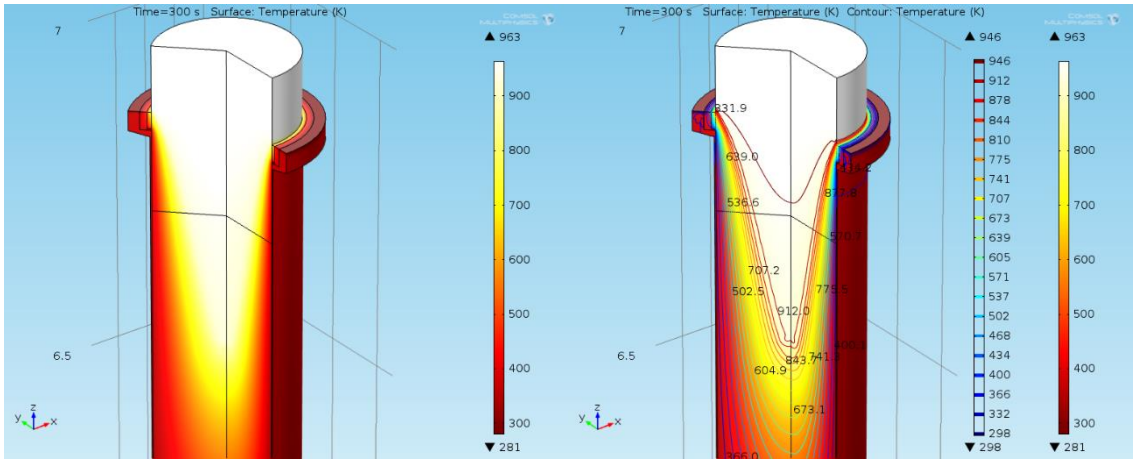

Figure 4.2: Steady state of DC cast billet sump profile corresponding to casting speed of 300 mm/min.

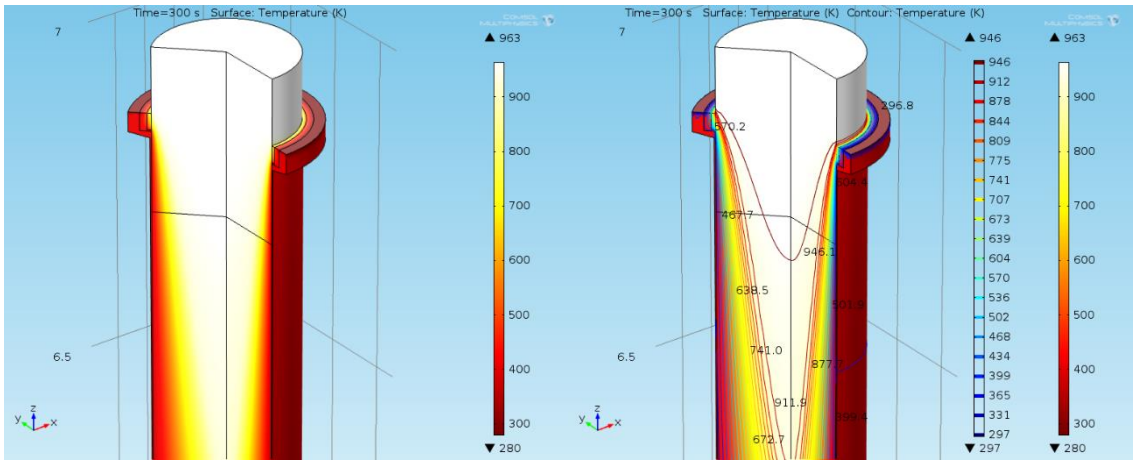

Figure 4.3: Steady state of DC cast billet sump profile corresponding to casting speed of 500 mm/min.

4.2.2 Effect of Rotor Speed on the Sump Profile

In this study, the influence of shearing device on the evolution of the sump profiles were revealed. In an industrial scale of billet size (206 mm in diameter; 7000 mm in length), a rotor-stator shearing device was immersed in between the graphite lining and wagstaff mould of the DC caster which was located in the billet top during the process, herein, termed as MC-DC casting. Many researches have been done and proven that the MC-DC technique on the semi-solid slurry promotes the grain refinements, and then delivered along the caster continuously **[3-10, 20, 40]**. However, the effect of the rotor speed during high casting speed was not reported in the literature, hence it is still unknown.

Earlier literature has revealed that the effect of high casting speed such as 300 mm/min did not provide a significant grain refined on the microstructure by using MC-DC technique **[10]**. However, the manipulation on the rotor speed has not been revealed yet. This is most probably due to insufficient time for primary cooling and the cast billet remain un-sheared as casting speed increase at constant rotor speed. Therefore, by increasing the rotor speed, a significant reduction in the billet sump has been spotted and as illustrated in **Figure 4.4, 4.5, 4.6, 4.7, and 4.8**.

Furthermore, to highlight the outcome, the DC caster with a shearing device was turned “OFF” during the casting process as illustrated in **Figure 4.4**. After that, the shearing device was turned “ON” and the speeds were slightly increased from 100 rpm to 200 rpm and 300 rpm in the COMSOL software environment. As the speed increases, **Figure 4.5** shown that the liquid sump are slightly decreases during the rotor speed of 50 rpm. Besides that, **Figure 4.6, 4.7, and 4.8**, have clearly demonstrated the evolution of the sump profiles and the shell wall thickness of the billets cast as the rotor speed of rotor-stator based device launched at 100 rpm, 200 rpm and 300 rpm respectively.

In addition, the results also indicated that the isothermal region has been created in the billet sump by MC-DC technique. Unlike the conventional type of direct chill casting which possess a huge temperature gradient that fluctuated in the billet sump. Hence, the phenomena have led to the irregularity of heat and mass transfer in the DC billet sump **[9, 10]**.

Earlier reports also proven that the heterogeneous solidification has provided by the dispersed oxide particles due to highly intensive shear of forced convection flow **[4]**. Nevertheless, the mechanism of nucleation growth still remain unclear until lately, some research have proven that the fragmented dendrites potent the nuclei growth under severe forced convection in the MC-DC casting technique **[9, 10, 12, 21]**.

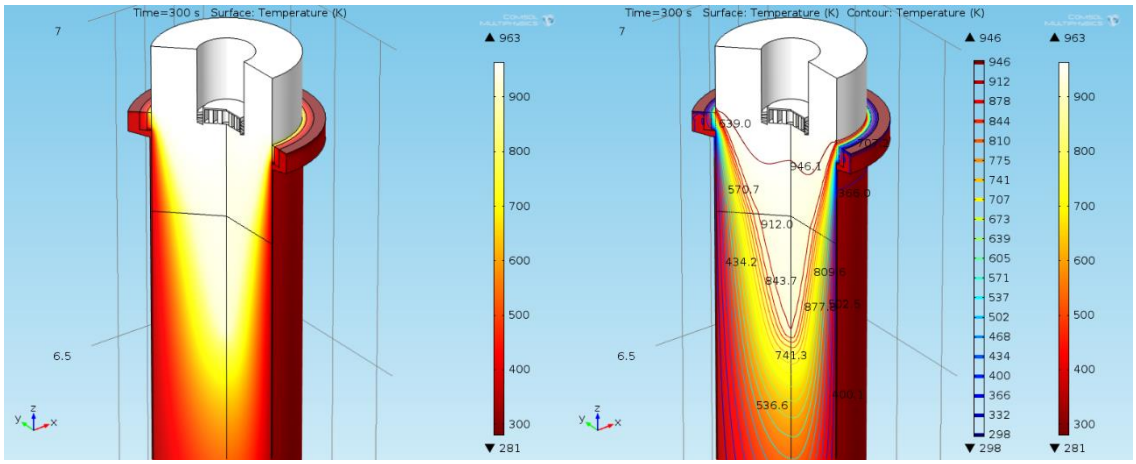

Figure 4.4: Steady state of MC-DC cast billet sump profile corresponding to casting speed of 300 mm/min with rotor speed of 0 rpm, where the device diameter is 80 mm and located at 110 mm depth.

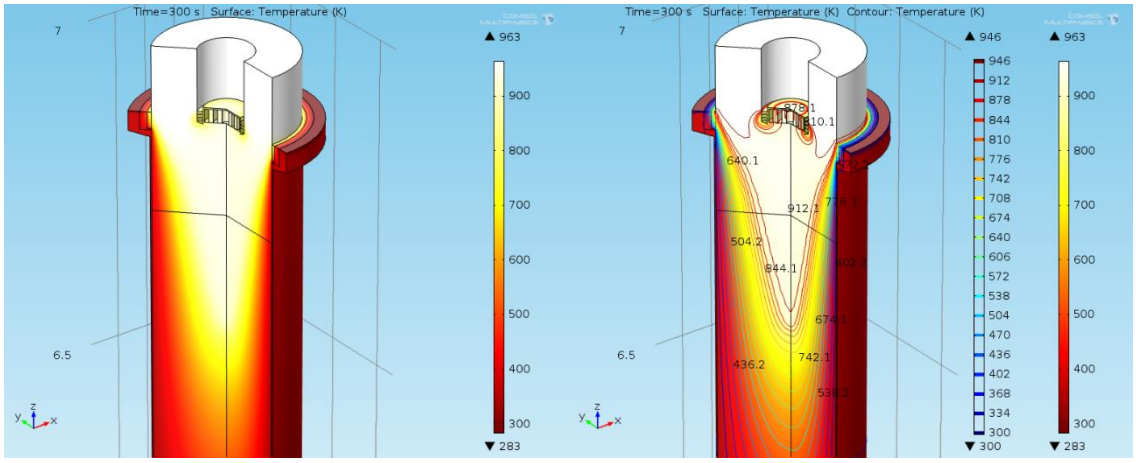

Figure 4.5: Steady state of MC-DC cast billet sump profile corresponding to casting speed of 300 mm/min with rotor speed of 50 rpm, where the device diameter is 80 mm and located at 110 mm depth.

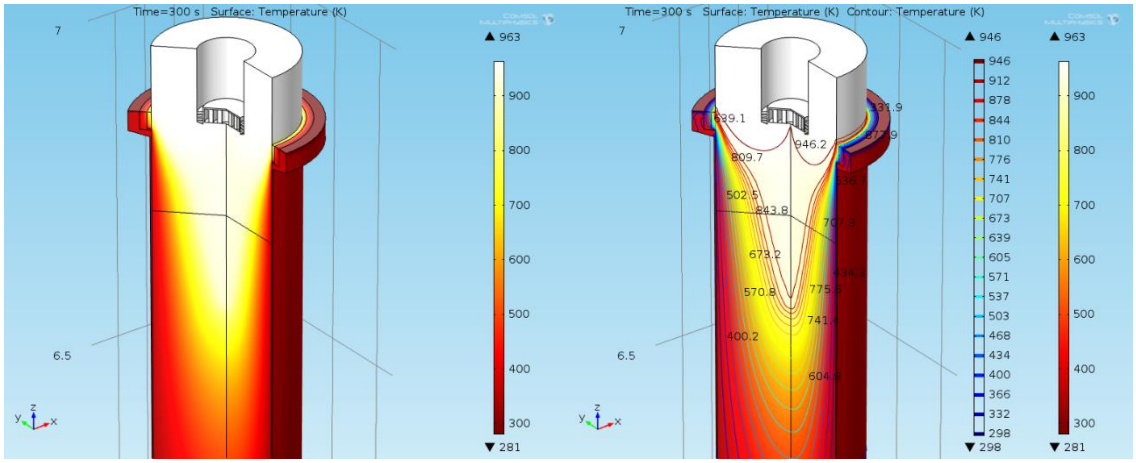

Figure 4.6: Steady state of MC-DC cast billet sump profile corresponding to casting speed of 300 mm/min with rotor speed of 100 rpm, where the device diameter is 80 mm and located at 110 mm depth.

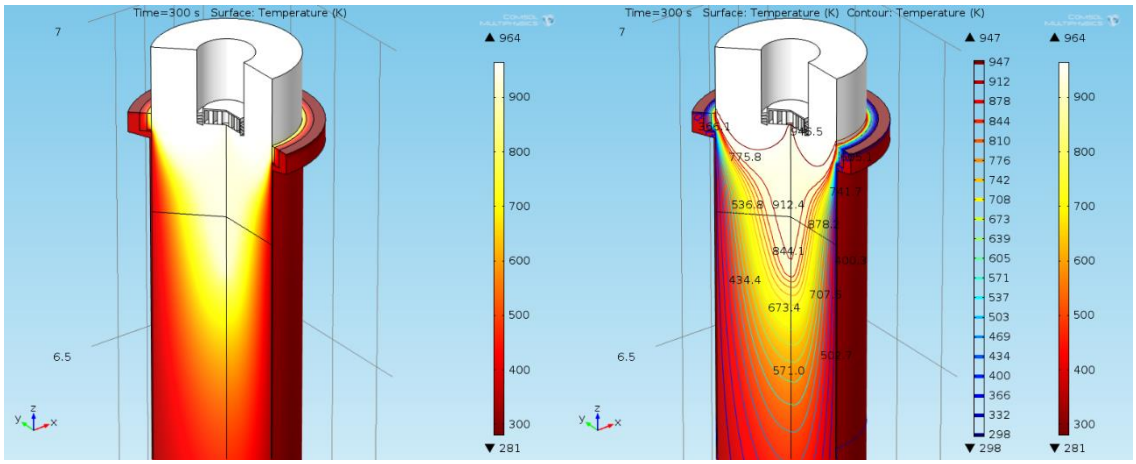

Figure 4.7: Steady state of MC-DC cast billet sump profile corresponding to casting speed of 300 mm/min with rotor speed of 200 rpm, where the device diameter is 80 mm and located at 110 mm depth.

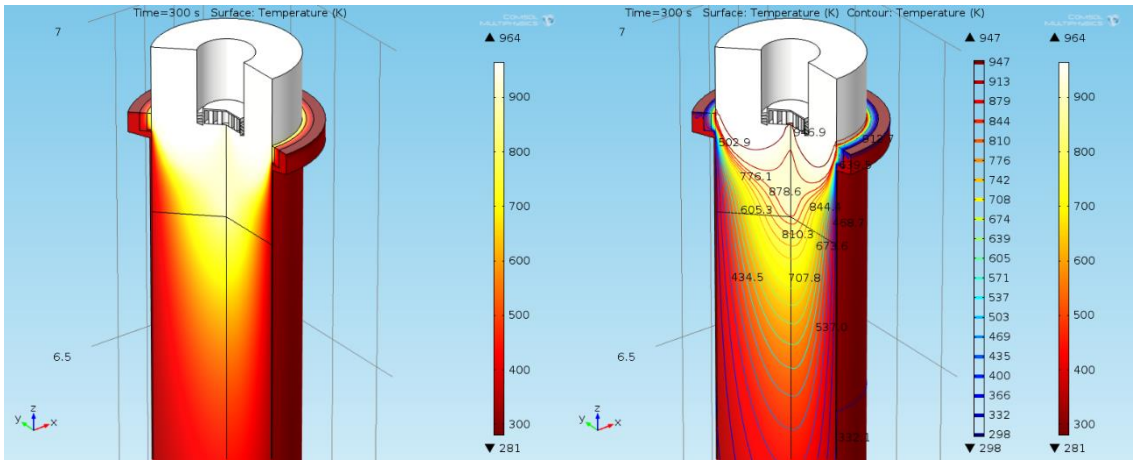

Figure 4.8: Steady state of MC-DC cast billet sump profile corresponding to casting speed of 300 mm/min with rotor speed of 300 rpm, where the device diameter is 80 mm and located at 110 mm depth.

4.2.3 Effect of Device Depth on the Sump Profile

In this study, the depth of shearing device immersion has been studied on the evolution of the sump profiles. The same technique was adopted, MC-DC technique to cast an industrial scale of billet size (206 mm in diameter; 7000 mm in length). Many researches have proven the effect of grain refinement and the solute distribution in the MC-DC cast billet **[3-10,12]**. However, the effect of the device depth on the temperature distribution sump profile was not reported in the literature, hence it is still unknown. In **Figure 4.9 (a, b)** illustrated the position of shearing device in two different cases to study the heat distribution in the billet sump.

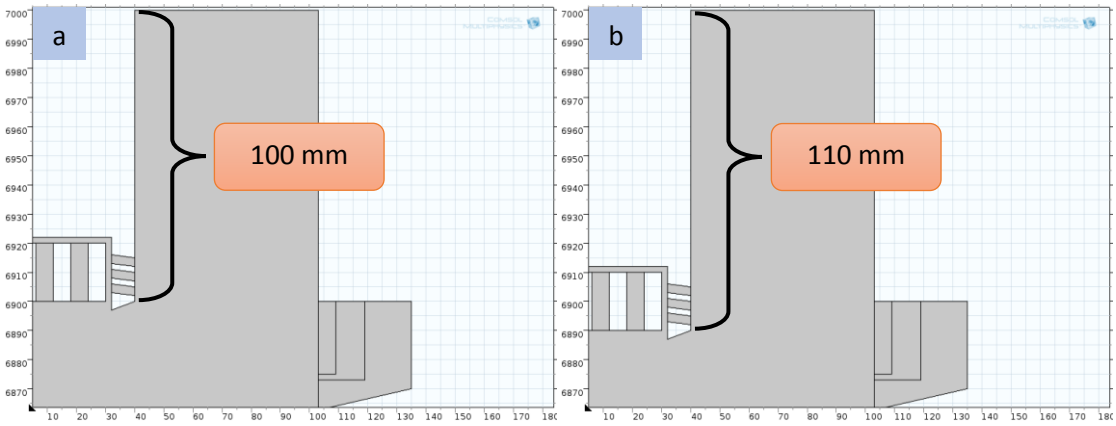

Figure 4.9: Position of device immersion during MC-DC billet casting at the depth of **(a)** 100 mm, and **(b)** 110 mm.

In **Figure 4.10** illustrated two MC-DC cast billet sump profiles with different depth of shearing device immersion that both rotor speed at 300 rpm under same casting speed, 300 mm/min. **Figure 4.10 (b)** shows the MC-DC billet casts with a shearing device that immersed in 110 mm depth appeared to have a shallower temperature sump profile compared to the 100 mm depth of device immersion of MC-DC billet cast in **Figure 4.10 (a)**. This was because at 110 mm depth of immersion, the rotor-stator device was nearer to the solid-liquid interface. As the rotor-stator based melt conditioning shearing device was turned "ON", a forced convection was generated to perform a stirring action above the solidification front of the billet sump. Therefore, results in substantial of dendrites fragmentation and uniform solute distribution across the sump of billet **[9]**.

Moreover, literature has revealed that once the shearing device was turned "ON", the huge temperature gradients tends to drop significantly and keep constant once the

melt conditioned regime was achieved. Furthermore, the temperature of molten alloys was just dropped at below the liquidus of the alloys, this was due to the fragmented dendrites by intensive shearing effect, leading to solid-liquid interface in isothermal regime **[8, 9]**. Therefore, the nearer the device to the solid fronts as depicted in **Figure 4.10 (b)**, more semi-solid has been sheared by the rotor-stator device and leading to achieve isothermal regime or lower temperature gradient compared to the further rotor-stator device from solid-liquid interface as shown in **Figure 4.10 (a)**. In other words, the depth of liquid sump is increased, because, the solid-liquid interface is far away from the tip of the device. Hence, the liquid sucked from the bottom will be hotter that in the earlier case, causing the time for nucleation growth has been slightly extended. The isothermal contours of the MC-DC casting with difference depths of the device are shown in **Figure 4.11**.

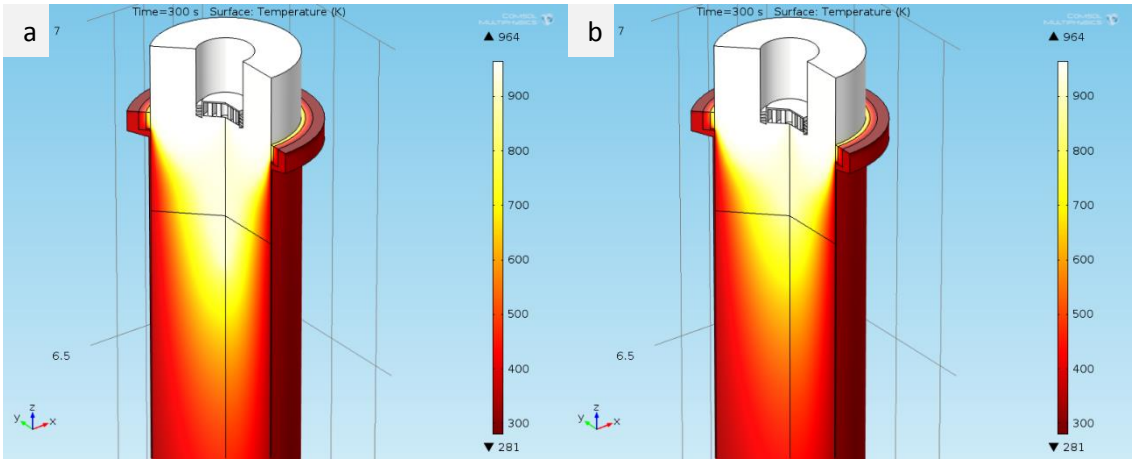

Figure 4.10: Comparison between device depth of **(a)** 100 mm, and **(b)** 110 mm at 300 rpm under 300 mm/min of casting speed.

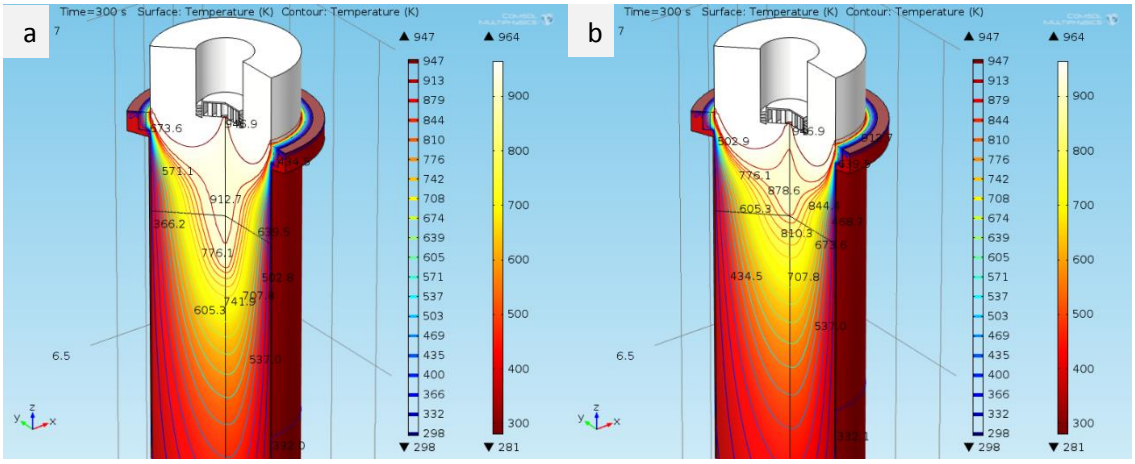

Figure 4.11: Isothermal contour of the comparison between device depth of **(a)** 100 mm, and **(b)** 110 mm at 300 rpm under 300 mm/min of casting speed.

On the other hands, the effect of rotor speed has been tested on the shallower device depth, which was 100 mm of immersion in the caster as depicted in **Figure 4.9 (a)**. The simulated results present a positive response towards the depth minimization of the billet sump as illustrated in **Figure 4.12, 4.13, 4.14, 4.15, and 4.16**. Under casting speed of 300 mm/min with 80mm in diameter of shearing device, the MC-DC casting processes were tested with varies rotor speed, such as 0 rpm, 50 rpm, 100 rpm, 200 rpm and 300 rpm accordingly. Finding results have proven that the increasing in rotor speed parameter able to minimize the gradient of temperature distribution in the billet sump in the case of MC-DC technique when compared to the DC casting process as shown in **Fig. 4.2**. With the helps in a thicker shell wall due to higher rotor speed, it is important for understanding the behaviour of hot-tears, cold-shut, and bleed-out in DC casting **[12]**.

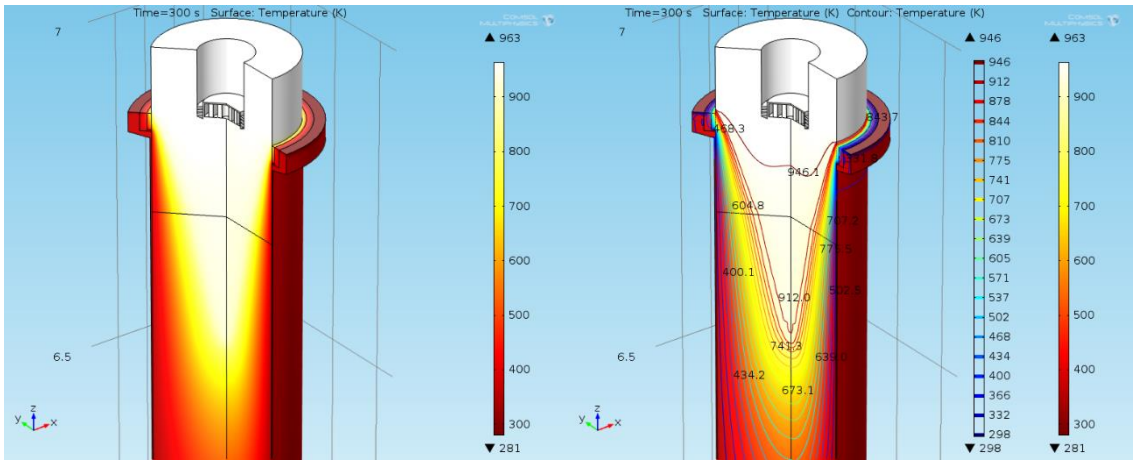

Figure 4.12: Steady state of MC-DC cast billet sump profile corresponding to casting speed of 300 mm/min with rotor speed of 0 rpm, where the device diameter is 80 mm and located at 100 mm depth.

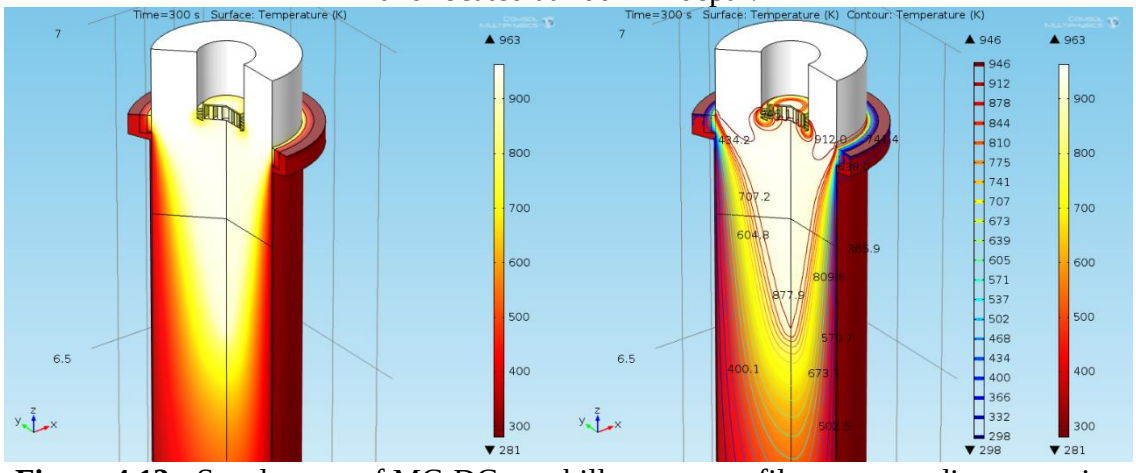

Figure 4.13: Steady state of MC-DC cast billet sump profile corresponding to casting speed of 300 mm/min with rotor speed of 50 rpm, where the device diameter is 80 mm and located at 100 mm depth.

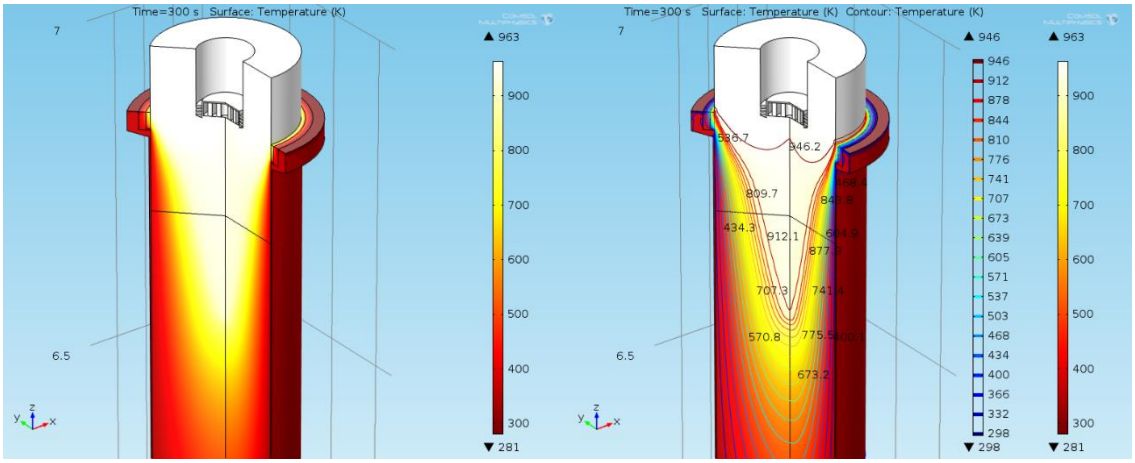

Figure 4.14: Steady state of MC-DC cast billet sump profile corresponding to casting speed of 300 mm/min with rotor speed of 100 rpm, where the device diameter is 80 mm and located at 100 mm depth.

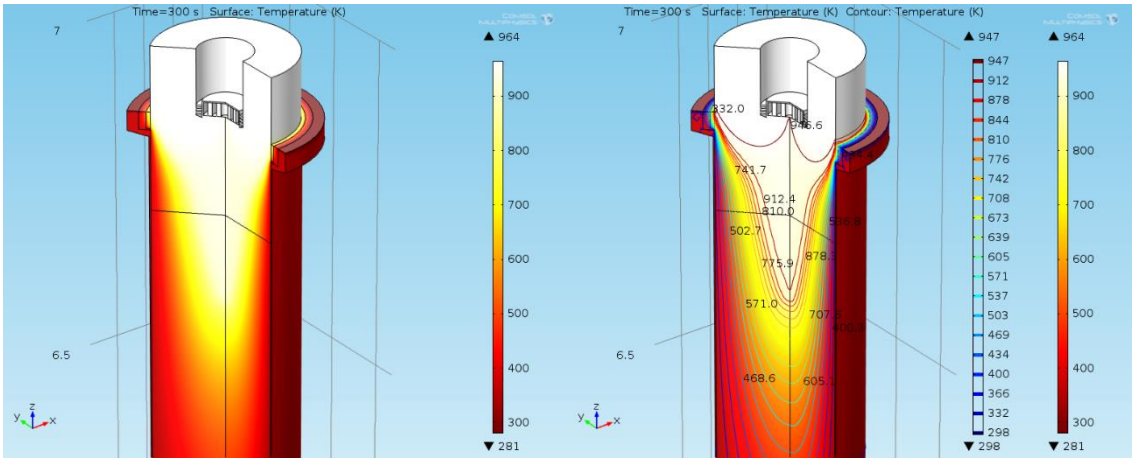

Figure 4.15: Steady state of MC-DC cast billet sump profile corresponding to casting speed of 300 mm/min with rotor speed of 200 rpm, where the device diameter is 80 mm and located at 100 mm depth.

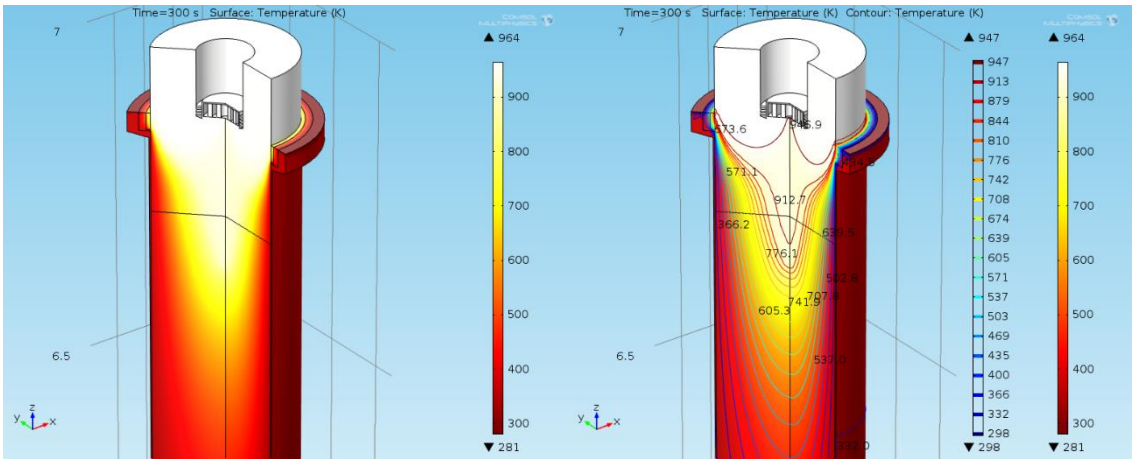

Figure 4.16: Steady state of MC-DC cast billet sump profile corresponding to casting speed of 300 mm/min with rotor speed of 300 rpm, where the device diameter is 80 mm and located at 100 mm depth.

4.2.4 Effect of Device Diameter on the Sump Profile

In this section, the effect of device diameter on the sump profile has been discussed. There were many literatures presented about the effect of MC-DC casting on grain refinement and the effect of water cooling on the cast billet surface. However, the effect of the device diameter was not reported yet, hence it is an interesting topic to be revealed. It is the first time that the study on the effect of device diameter are formed.

The results have been demonstrated in **Figure 4.17 (a)** a 40 mm diameter of rotor-stator shearing device and **Figure 4.17 (b)** an 80 mm diameter of rotor-stator shearing device under casting speed of 300 mm/min in an industrial scale of billet size (206 mm in diameter; 7000 mm in length). Based on the results, the smaller rotor diameter appeared to have higher suction force compared to the bigger rotor diameter. Hence, lead to a shallower depth of billet sump, which also influence the temperature gradient of the casting process.

According to the law of conservation of mass, the principle states that mass cannot be created or destroyed during a process. During a steady flow process, the amount of mass flow into a control volume is equal to the amount of mass flow out of a control volume. Thus, the mass conservation law also called the equation of continuity and can be expressed as Eq. (4.1)

$$\dot{m} = \rho V A \tag{4.1}$$

where, $\dot{m}$ is the mass flow rate ($kg.s^{-1}$), ρ is the density ($kg.m^{-3}$), V is the average flow velocity ($m.s^{-1}$), and A is the cross-sectional area of the medium (m^2). In the case of large device as shown in **Figure 4.17 (b)**, the area of cross-section of the device is large. Therefore, the suction velocity will be decreased in order to keep the mass flow rate constant. According to the mass continuity equation, the liquid state of AZ31 Mg-alloy is incompressible and density of the molten melt is uniform during the casting process. Hence, the equation in Eq. (4.1) can be expressed as Eq. (4.2)

$$Q = V_1 A_1 = V_2 A_2 = constant \tag{4.2}$$

where, Q is volume flow rate ($m^3.s^{-1}$) which remain constant , V_1 is the average flow velocity of the liquid in the large device ($m.s^{-1}$), and $A_1$is the cross-sectional area of the large device (m^2), V_2 is the average flow velocity of the liquid in the small device

($m.s^{-1}$), and A_2 is the cross-sectional area of the small device (m^2). In other word, the small device diameter as shown in **Figure 4.17 (a)**, has higher suction velocity due to the small cross-sectional area of the smaller device in order to keep the mass flow rate constant. Therefore, the device with larger diameter (80 mm), sucks the liquid with a lower velocity than in the case of smaller device diameter (40 mm).

Furthermore, according to the physics of kinetic energy equation, a work is done by a body of given mass with respect to the stated velocity. The kinetic energy is expressed as Eq. (4.3)

$$E_k = \frac{1}{2}\, mv^2 \tag{4.3}$$

where, E_k is kinetic energy (J), m is the mass of an object (kg), and v is the velocity of the system ($m.s^{-1}$). In the study, the smaller rotor-stator device possess higher suction velocity in the billet sump, which eventually leads to intensive dendrite fragmentation than in the case of larger rotor-stator device. Hence, the sump profile sump profile appeared shallower compared the larger rotor-stator device. This is due to the fact that, higher suction velocity contributes higher kinetic energy. (Xia et al., 2013) and (Prasada Rao, 2014) reported that the gradient of temperature distribution in the billet sump drops abruptly in the MC-DC regime and just below the liquidus of the alloy during forced convection shearing **[7,9]**. From the **Figure 4.18 (a)**, the temperature at the tip of the 40 mm diameter of rotor-stator device is 845.10 K (571.95 ℃) which is far less than the liquidus temperature of AZ31 Mg-alloy at 903.15 K (630.00 ℃). While compared to the **Figure 4.18 (b)**, the temperature below the rotor-stator device is at 878.6 K (605.45 ℃), which is hotter than the previous case of smaller rotor-stator device. Which clearly proves that the solid-fraction in the billet sump in the case of 40 mm diameter of MC-DC device is higher than in the case of the 80 mm diameter of MC-DC device. Which is due to less-intensive dendrite fragmentation in the case of the 80 mm device, owing to its low kinetic energy.

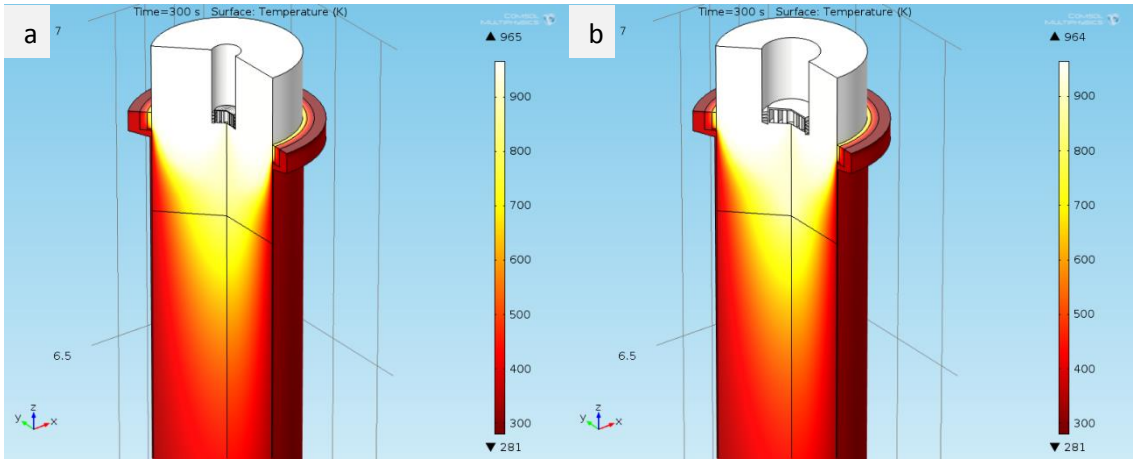

Figure 4.17: Comparison between device diameter of **(a)** 40 mm, and **(b)** 80 mm at 300 rpm under 300 mm/min of casting speed.

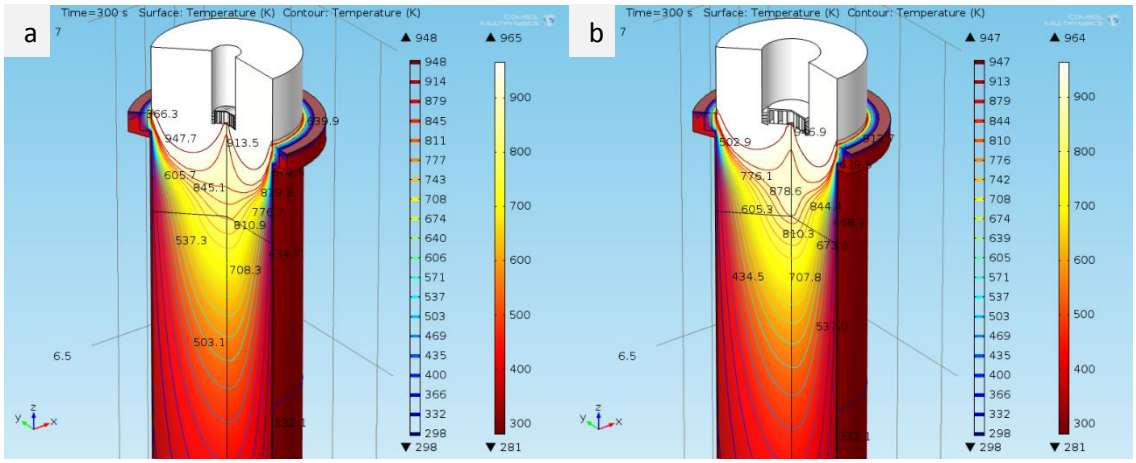

Figure 4.18: Isothermal contour of the comparison between device diameter of **(a)** 40 mm, and **(b)** 80 mm at 300 rpm under 300 mm/min of casting speed.

4.3 SUMMARY

Present work has discussed the four different cases based on the effect of various parameters, such as casting speed, rotor speed, depth of rotor-stator device and diameter of rotor-stator device. The presented results and discussions are very useful for the industry to have the reference for parameters optimization, so that, the behaviour of various defects such as bleed-outs, cold-shuts and other defects in the DC casting can be predicted through temperature distribution.

CHAPTER 5

CONCLUSIONS AND RECOMMENDATIONS

5.1 INTRODUCTION

The purpose of this chapter is to outline the significant effect on various parameters such as casting speed, rotor speed, depth of rotor-stator device and diameter of rotor-stator device on an industrial scale of DC cast billet. Follow on, the recommendations and suggestions for future work of this work are to be discussed.

5.2 CONCLUSIONS

In this project, all the objectives were achieved, where the numerical model of DC caster and MC-DC caster were designed and developed by using COMSOL Multiphysics. The problems were solved based on the heat transfer module and fluid flow module, in order to investigate the influence of various parameters such as casting speed, rotor speed, depth of shearing device and diameter of shearing device on an industrial scale of billet cast in diameter of 206 mm and a length of 7000 mm.

By investigation, the effect of various parameters on the billet sump profile, the solidification behaviour of the AZ31 Mg-alloy cast billets have been justified. The results presented that the temperature gradient in the sump of the MC-DC caster has been minimized significantly when compared to the conventional DC caster. Additionally, the results also revealed that the high intensive shearing device with various rotor speed able to manipulate the depth of liquid sump. Meanwhile, the efficiency and productivity were influenced by the rotor-stator depth and diameter. In

the study of device's depth, the shorter the distance between the solid-liquid interface and the tip of rotor-stator device, the lesser the depth of sump. This is due to the cooler liquid has been sucked up and ruptured by shearing device, in order to achieve an isothermal regime in short time. Hence, the forcibly circulation on the solid-liquid interface has led to dendrites fragmentation, which promote grain refinements. Lastly, the rotor-stator device with smaller device diameter, sucks the liquid melts with a higher velocity, which results to intensive dendrites fragmentation. Thus, sump profile appeared shallower compared to the larger diameter of rotor-stator device. Eventually, it is noted that the isothermal regime in the billet sump has been created under the MC-DC process.

In a nutshell, this project has provided the information on the effect of various parameters on MC-DC casting technique. These simulation results revealed the reasonable agreement with the experiments conducted in previous experimental based literature. Findings of the work help in understanding the effect of various process parameters on the billet sump of DC casting and MC-DC casting, and to find the optimum conditions without performing actual casting experiments which is costly. The presented results and discussions are very useful for the industry to have reference and analysis in order to obtain the optimal parameters and minimize the defects.

5.3 FUTURE WORK RECOMMENDATIONS

The present work has successfully designed and developed the model for DC and MC-DC casting for simulation created by COMSOL Multiphysics and the effect of various parameters were studied and discussed for the first time. It might have certain imperfections, where at some point it can be improved in future work. Therefore, the following recommendations can be considered in future research in order to obtain more accurate results.

- The modelling of the effects of the various parameters presented in this work, although the thermal-solute distributions of the material is not presented together with the sump profile, but the trends of the heat transfer that cause by the variations of the device parameters can be predicted. Therefore, the work can be improved by

study the chemical composition in the billet sump, which promote a better understanding on the behaviour of macrosegregation.

- Moreover, it can be a more complex work, but it is more interesting to model the rotor-stator device by using 3D geometry instead of 2D axis symmetry model. Thus, through this approach, the hypothetical shearing device can be replaced by a 3D rotating device which provide more accurate results.

REFERENCES

[1] Grandfield, J., Eskin, D. G., & Bainbridge, I. (2013). *Direct-chill casting of light alloys: science and technology*. John Wiley & Sons.

[2] Eskin, D. G. (2008). *Physical metallurgy of direct chill casting of aluminum alloys*. CRC press.

[3] Haghayeghi, R., Liu, Y., & Fan, Z. Y. (2008). Melt Conditioned Direct Chill Casting (MC-DC) of Wrought Al-Alloys. *Solid State Phenomena*, *141-143*, 403–408. http://doi.org/10.4028/www.scientific.net/SSP.141-143.403

[4] Fan, Z., Xia, M., Zhang, H., Liu, G., Patel, J. B., Bian, Z., … Scamans, G. M. (2009). Melt conditioning by advanced shear technology (MCAST) for refining solidification microstructures. *International Journal of Cast Metals Research*, *22*(1-4), 103–107. http://doi.org/10.1179/136404609X367443

[5] Zuo, Y., Li, H., Xia, M., Jiang, B., Scamans, G. M., & Fan, Z. (2011). Refining grain structure and porosity of an aluminium alloy with intensive melt shearing. *Scripta Materialia*, *64*(2), 209–212. http://doi.org/10.1016/j.scriptamat.2010.09.046

[6] Zuo, Y. B., Jiang, B., Zhang, Y., & Fan, Z. (2012). Grain refinement of DC cast magnesium alloys with intensive melt shearing. *IOP Conference Series: Materials Science and Engineering*, *27*(1), 12043. http://doi.org/10.1088/1757-899X/27/1/012043

[7] Xia, M. X., Prasada Rao, A. K., & Fan, Z. Y. (2013). Solidification Mechanisms in Melt Conditioned Direct Chill (MC-DC) Cast AZ31 Billets. *Materials Science Forum*, *765*, 291–295. http://doi.org/10.4028/www.scientific.net/MSF.765.291

[8] Jones, S., Prasada Rao, A. K., & Fan, Z. (2013). Melt Conditioned Direct Chill (MC-DC) Casting of Al Alloys. *Transactions of the Indian Institute of Metals*, *66*(2), 117–121. http://doi.org/10.1007/s12666-012-0235-5

[9] Prasada Rao, A. K. (2014). Understanding the Evolution of the Microstructure in Melt-Conditioned Direct-Chill Cast Al Alloys. *Materials and Manufacturing Processes*, *29*(7), 848–852. http://doi.org/10.1080/10426914.2014.921698

[10] Prasada Rao, A. K. (2015). Nucleation in Al Alloys Processed By MCDC Casting. *Journal of Materials Engineering and Performance*, *24*(6), 2219–2224. http://doi.org/10.1007/s11665-015-1463-8

[11] Baserinia, A. R., Ng, H., Weckman, D. C., Wells, M. A., Barker, S., & Gallerneault, M. (2012). A Simple Model of the Mold Boundary Condition in Direct-Chill (DC) Casting of Aluminum Alloys. *Metall. Mater. Trans. B*, *43*(4), 887–901. http://doi.org/10.1007/s11663-012-9658-y

[12] Walinjkar, D., & Rao, A. K. P. (2015). C-DC and MC–DC casting of Al-alloys – A comsol approach. *Materials Letters*, *161*, 698–700. http://doi.org/10.1016/j.matlet.2015.09.082

[13] Begum, L., & Hasan, M. (2014). 3-D CFD simulation of a vertical direct chill slab caster with a submerged nozzle and a porous filter delivery system. *International Journal of Heat and Mass Transfer*, *73*(JUNE 2014), 42–58.

http://doi.org/10.1016/j.ijheatmasstransfer.2014.01.072

[14] Sengupta, J., Thomas, B. G., & Wells, M. A. (2005). The use of water cooling during the continuous casting of steel and aluminum alloys. *Metallurgical and Materials Transactions A*, *36*(1), 187–204. http://doi.org/10.1007/s11661-005-0151-y

[15] Caron, E. J. F. R., Baserinia, A. R., Ng, H., Wells, M. A., & Weckman, D. C. (2012). Heat-Transfer Measurements in the Primary Cooling Phase of the Direct-Chill Casting Process. *Metallurgical and Materials Transactions B*, *43*(5), 1202–1213. http://doi.org/10.1007/s11663-012-9688-5

[16] Eskin, D. G., Du, Q., & Katgerman, L. (2006). Relationship between shrinkage-induced macrosegregation and the sump profile upon direct-chill casting. *Scripta Materialia*, *55*(8), 715–718. http://doi.org/10.1016/j.scriptamat.2006.06.021

[17] Nadella, R., Eskin, D. G., Du, Q., & Katgerman, L. (2008). Macrosegregation in direct-chill casting of aluminium alloys. *Progress in Materials Science*, *53*(3), 421–480. http://doi.org/10.1016/j.pmatsci.2007.10.001

[18] Suyitno, Eskin, D. G., & Katgerman, L. (2006). Structure observations related to hot tearing of Al–Cu billets produced by direct-chill casting. *Materials Science and Engineering: A*, *420*(1-2), 1–7. http://doi.org/10.1016/j.msea.2005.12.037

[19] Hatami, N., Babaei, R., Dadashzadeh, M., & Davami, P. (2008). Modeling of hot tearing formation during solidification. *Journal of Materials Processing Technology*, *205*(1-3), 506–513. http://doi.org/10.1016/j.jmatprotec.2007.11.260

[20] Haghayeghi, R., Zoqui, E. J., Green, N. R., & Bahai, H. (2010). An investigation on DC casting of a wrought aluminium alloy at below liquidus temperature by using melt conditioner. *Journal of Alloys and Compounds*, *502*(2), 382–386. http://doi.org/10.1016/j.jallcom.2010.04.173

[21] Flemings, M.C. (1991). Behavior of metal alloys in the semisolid state. *Metallurgical Transactions A, 22*, 957-981.

[22] COMSOL Multiphysics. (2015, October 11). In *Wikipedia, The Free Encyclopedia*. Retrieved 14:34, November 13, 2015, from https://en.wikipedia.org/w/index.php?title=COMSOL_Multiphysics&oldid=685197082

[23] Sabau, A. et al., 2004. Heat transfer boundary conditions for the numerical simulation of the DC casting process. In *TMS Light Metals*. pp. 667–672. Available at: http://www.scopus.com/inward/record.url?eid=2-s2.0-2442428626&partnerID=tZOtx3y1.

[24] Baserinia, A.R. et al., 2012. A Simple Model of the Mold Boundary Condition in Direct-Chill (DC) Casting of Aluminum Alloys. *Metall. Mater. Trans. B*, 43(4), pp.887–901. Available at: http://link.springer.com/10.1007/s11663-012-9658-y.

[25] Hu, H., Zhang, D. & Yang, M., 2008. Numerical simulation of thermal stress in cast billets made of AZ31 magnesium alloy during direct-chill casting. *Journal of Manufacturing Processes*, 10(2), pp.82–88. Available at: http://linkinghub.elsevier.com/retrieve/pii/S1526612509000115.

[26] Hu, W. et al., 2013. Numerical simulation of DC casting of AZ31 magnesium slab

at different casting speeds. *Journal of Magnesium and Alloys*, 1(1), pp.88–93. Available at: http://linkinghub.elsevier.com/retrieve/pii/S221395671300011X.

[27] Hasan, M., & Begum, L., 2014. On numerical modeling of low-head direct chill ingot caster for magnesium alloy AZ31. *Journal of Magnesium and Alloys*, *2*(4), 275–286. http://doi.org/10.1016/j.jma.2014.11.008

[28] Hao, H. et al., 2004. Development and validation of a thermal model of the direct chill casting of AZ31 magnesium billets. *Metallurgical and Materials Transactions A*, 35(12), pp.3843–3854.

[29] Ameur, H. & Bouzit, M., 2012. Mixing in shear thinning fluids.pdf. *Brazilian Journal of Chemical Engineering*, 29(2), pp.349–358.

[30] Ameur, H. & Bouzit, M., 2013. Numerical investigation of flow induced by a disc turbine in unbaffled stirred tank. *Acta Scientiarum. Technology*, 35(3), pp.469–476. Available at: http://periodicos.uem.br/ojs/index.php/ActaSciTechnol/article/view/15554.

[31] FAN, J., WANG, Y. & FEI, W., 2007. Large Eddy Simulations of Flow Instabilities in a Stirred Tank Generated by a Rushton Turbine. *Chinese Journal of Chemical Engineering*, 15(2), pp.200–208.

[32] Nurtono, T. et al., 2009. Macro-instability characteristic in agitated tank based on flow visualization experiment and large eddy simulation. *Chemical Engineering Research and Design*, 87(7), pp.923–942.

[33] Jafari, A. et al., 2010. Numerical modeling of macrosegregation during the direct-chill casting of an alalloy billet. *Iranian Journal of Materials Science and Engineering*, 7(3), pp.39–50.

[34] M'Hamdi, M. & Mo, A., 2005. On modelling the interplay between microporosity formation and hot tearing in aluminium direct-chill casting. *Materials Science and Engineering A*, 413-414, pp.105–108.

[35] Shi, S. et al., 2009. A 3-D Mathematical Model of Thermal Field Evolution in the Direct Chill Casting of Superlight Magnesium Alloy Slabs. *Rare Metal Materials and Engineering*, 38(2), pp.203–208. Available at: http://linkinghub.elsevier.com/retrieve/pii/S1875537210600197.

[36] Založnik, M. & Šarler, B., 2005. Modeling of macrosegregation in direct-chill casting of aluminum alloys: Estimating the influence of casting parameters. *Materials Science and Engineering: A*, 413-414, pp.85–91. Available at: http://linkinghub.elsevier.com/retrieve/pii/S0921509305011172.

[37] Hao, H. et al., 2007. Improvement of Casting Speed and Billet Quality of Direct Chill Cast Aluminum Wrought Alloy with Combination of Slit Mold and Electromagnetic Coil. *Materials Transactions*, 48(8), pp.2194–2201. Available at: http://joi.jlc.jst.go.jp/JST.JSTAGE/matertrans/MRA2007030?from=CrossRef.

[38] Du, Q., Eskin, D.G. & Katgerman, L., 2005. The effect of ramping casting speed and casting temperature on temperature distribution and melt flow patterns in the sump of a DC cast billet. *Materials Science and Engineering A*, 413-414, pp.144–150.

[39] Hasan, M. & Begum, L., 2015. Semi-continuous casting of magnesium alloy AZ91 using a filtered melt delivery system. *Journal of Magnesium and Alloys*, 3(4), pp.283–301. Available at: http://linkinghub.elsevier.com/retrieve/pii/S2213956715000791.

[40] ZHU, G. et al., 2010. Effect of high shear rate on solidification microstructure of semisolid AZ91D alloy. *Transactions of Nonferrous Metals Society of China*, 20, pp.s868–s872. Available at: http://linkinghub.elsevier.com/retrieve/pii/S1003632610605973.

APPENDIX A

GANTT CHARTS

Gantt chart for FYP 1

No.	Activities / Tasks	Action	Week Duration for FYP 1 (8 Sept 2015 to 18 Dec 2015)													
			1	2	3	4	5	6	7	8	9	10	11	12	13	14
1	Briefing on FYP1	Plan														
		Complete														
2	Meeting with Supervisor	Plan														
		Complete														
3	Research on Topic and Literature Review	Plan														
		Complete														
4	Casting Parameters Configuration	Plan														
		Complete														
5	Generate Project Proposal	Plan														
		Complete														
6	Project Proposal Submission	Plan														
		Complete														
7	Project Presentation FYP 1	Plan														
		Complete														
8	Report Writing	Plan														
		Complete														

Gantt chart for FYP 2

No.	Activities / Tasks	Action	Week Duration for FYP 2 (15 Feb 2016 to 27 May 2016)													
			1	2	3	4	5	6	7	8	9	10	11	12	13	14
1	Briefing on FYP2	Plan														
		Complete														
2	Meeting with Supervisor	Plan														
		Complete														
3	Literature Review	Plan														
		Complete														
4	Geometry Design for DC Caster	Plan														
		Complete														
5	Design Boundary Condition	Plan														
		Complete														
6	Simulation on DC and MC-DC caster	Plan														
		Complete														
7	Results and Discussion	Plan														
		Complete														
8	Thesis Writing	Plan														
		Complete														
9	Project Presentation FYP 2	Plan														
		Complete														
10	Thesis Compilation	Plan														
		Complete														